TITLE PAGE

Title: Engineered context-sensitive agonism – tissue-selective drug signaling through a G protein-coupled receptor

Authors: Wiebke K. Seemann[#], Daniela Wenzel, Ramona Schrage, Justine Etscheid, Theresa Bödefeld, Anna Bartol, Mareille Warnken, Philipp Sasse, Jessica Klöckner, Ulrike Holzgrabe, Marco DeAmici, Eberhard Schlicker, Kurt Racké, Evi Kostenis, Rainer Meyer, Bernd K. Fleischmann, and Klaus Mohr

Affiliations: Pharmacology and Toxicology Section, Institute of Pharmacy, University of Bonn, Bonn, Germany (W.K.S, R.S., J.E., T.B., A.B., K.M.); Institute of Physiology I, Life and Brain Center, University Clinic of Bonn, Bonn, Germany (D.W., P.S., B.K.F.); Institute of Pharmacology & Toxicology, University of Bonn, Bonn, Germany (M.W., E.S., K.R.); Department of Pharmaceutical Chemistry, Institute of Pharmacy, University of Würzburg, Würzburg, Germany (J.K., U.H.); Dipartimento di Scienze Farmaceutiche, Sezione di Chimica Farmaceutica 'Pietro Pratesi', Università degli Studi di Milano, Milano, Italy (M.D.); Molecular-, Cellular-, and Pharmacobiology Section, Institute of Pharmaceutical Biology, University of Bonn, Bonn, Germany (E.K.); Institute of Physiology II, University of Bonn, Bonn, Germany (R.M.); Department of Pharmacology, University of Cologne, Cologne, Germany (W.K.S.)

RUNNING TITLE PAGE

a) Running title: Context-sensitive agonism through a G protein-coupled receptor

b) Corresponding authors: Wiebke Kirsten Seemann

Institute of Pharmacy

Pharmacology and Toxicology Section

Gerhard-Domagk-Str. 3

University of Bonn, 53121 Bonn, Germany

Phone: +49 228 73 2293, +49 176 21218175

Fax: +49 228 73 9215

Email: seemannwiebke@web.de

Bernd K. Fleischmann

Institute of Physiology I

Life and Brain Center

Sigmund-Freud-Str. 25

University Clinic of Bonn, 53127 Bonn, Germany

Phone: +49 228 6885 200

Fax: +49 228 6885 201

Email: bernd.fleischmann@uni-bonn.de

c) Number of text pages: 23

Number of tables: none

Number of figures: 5

Number of references: 55

Number of words in the abstract: 144

JPET Fast Forward. Published on November 15, 2016 as DOI: 10.1124/jpet.116.237149
This article has not been copyedited and formatted. The final version may differ from this version.

Number of words in the introduction: 686

Number of words in the discussion: 1173

d) Non-standard abbreviations: ANOVA, one-way analysis of variance; CHO-hM_2, Chinese hamster ovary cells stably transfected with the human M_2 receptor; CNS, central nervous system; DMR, dynamic mass redistribution; E_{max}, maximal inducible effect; eCM, embryonic cardiomyocytes; FSK, forskolin; $G_{i/o}$, inhibitory G protein; G_s, stimulatory G protein; GPCR, G protein-coupled receptor; [^{3}H]NMS, [^{3}H]N-methylscopolamine bromide; IBMX, isobutylmethylxanthine; IC_{50}, inflection point of sigmoidal binding curves; I-6-p, iper-6-phth; I-8-p, iper-8-phth; ISO, isoprenaline; K_A, apparent binding constant; LVCM, left ventricular catheter measurements; mAChRs, muscarinic acetylcholine receptors; MRC-5, human lung fibroblasts; OxoM, oxotremorine M; Pilo, pilocarpine; tau (τ), operational efficacy

e) Recommended section: Cellular and Molecular

ABSTRACT

Drug discovery strives for selective ligands to achieve targeted modulation of tissue function. Here we introduce engineered context-sensitive agonism as a post-receptor mechanism for tissue-selective drug action through a G protein-coupled receptor. Acetylcholine M_2-receptor activation is known to mediate, among other actions, potentially dangerous slowing of the heart rate. This unwanted side effect is one of the main reasons that limit clinical application of muscarinic agonists. Herein we show that dualsteric (orthosteric/allosteric) agonists induce less cardiac depression ex vivo and in vivo than conventional full agonists. Exploration of the underlying mechanism in living cells employing cellular dynamic mass redistribution identified context-sensitive agonism of these dualsteric agonists. They translate elevation of intracellular cAMP into a switch from full to partial agonism. Designed context-sensitive agonism opens an avenue towards post-receptor pharmacological selectivity, which even works in target tissues operated by the same subtype of pharmacological receptor.

INTRODUCTION

Differences in structure between receptor subtypes allow for the design of subtype-selective drugs. In the present study we shift focus from differences in receptor structure towards differences in subsequent intracellular signal propagation to engender tissue-selectivity of drug action. This concept is also addressed as “cell-based functional selectivity” (Kenakin, 2007) or “phenotypic pharmacology” (Nelson and Challiss, 2007) and is based on the stoichiometry and sensitivity of the cellular components driving the cellular response. It should not be confounded with “receptor-based selectivity” or “ligand-induced bias” (Kenakin, 2007). In contrast to conventional binding selectivity, cell state-dependent signaling will generate selectivity even between tissues endowed with the same receptor subtype. For this principle to work it is crucial to chemically encode agonist sensitivity at a level that discriminates between different states of cellular activity. Such “chemically engineered” context-dependent signaling will be introduced here. As a paradigm we will elucidate why activation of the M_2 muscarinic acetylcholine receptor can be exploited to suppress pain (Matera et al., 2014), even though this subtype would in principle also mediate dangerous slowing of the heart rate.

Remarkably, even permanently charged muscarinic ligands unable to penetrate the blood-brain-barrier are powerful analgesics in animal experiments and such peripheral compounds lack unwanted central tremorgenic activity (Barocelli et al., 2001; Matera et al., 2014). Therefore, permanently charged M_2-selective agonists should be useful for the treatment of pain disorders. In mammalian hearts, M_2 receptor-signaling is preferentially mediated via activation of inhibitory G proteins ($G_{i/o}$), whereas counteracting adrenergic β-receptors activate stimulatory G protein (G_s) signaling (for reviews (Brodde and Michel, 1999; Haga, 2013)). This functional antagonism converges on the level of intracellular cAMP. Therefore, we hypothesized less effective cholinergic signaling by dualsteric agonists to occur in tissues

JPET Fast Forward. Published on November 15, 2016 as DOI: 10.1124/jpet.116.237149
This article has not been copyedited and formatted. The final version may differ from this version.

under conditions of elevated cAMP. This would allow the organism to maintain sufficient blood pressure in spite of muscarinic receptor activation.

In order to probe feasibility of this concept, we applied a novel type of agonist engineered to transduce receptor activation with down-tuned efficacy (Bock et al., 2012). These “dualsteric” (bitopic orthosteric/allosteric) ligands activate the receptor protein from the orthosteric transmitter binding site and simultaneously bind to the receptor’s allosteric vestibule thereby hindering the receptor from adopting the fully active state (supplementary Fig. S1, for review (Mohr et al., 2013)). The term "dualsteric" illustrates that ligand binding is present at two sites on one and the same receptor protein. For comparison, we included a conventional full agonist (oxotremorine M) and an archetypal weak partial agonist (pilocarpine).

Action of these tools was investigated in different M_2 receptor expression systems. First, we quantified ligand-induced G protein activation in [^{35}S]GTPγS binding experiments performed with membrane homogenates of Chinese hamster ovary cells stably transfected with the human M_2 receptor (CHO-hM_2). To illustrate the influence of the cellular context on compound-induced receptor signaling, we, second, applied murine hippocampal brain slices to detect ligand-induced inhibition of acetylcholine release via presynaptic inhibitory M_2 receptors. Third, we analyzed the negative chronotropic response in spontaneously beating murine embryonic cardiomyocytes (eCM) after agonist application. The orthosteric agonist oxotremorine M (OxoM), the dualsteric agonist iper-6-phth (I-6-p) and the partial agonist pilocarpine (Pilo) did not fully inhibit acetylcholine release from cholinergic nerve endings of the hippocampus. In contrast to this, all compounds induced full intrinsic efficacy in eCM, i.e. complete silencing of spontaneous beating. The intensity of drug action is well known to depend on the level of receptor expression (Kenakin, 2007; Rajagopal et al., 2011). However, the functional status of the receptor protein may be also critical. Here, we show that the intrinsic efficacy of the dualsteric compound for slowing spontaneously beating of eCM declines with elevated intracellular cAMP. Additionally, left ventricular catheter

measurements (LVCM) in anesthetized mice disclose strongly improved cardiac tolerability of the applied dualsteric agonist compared with the conventional orthosteric agonist OxoM. To validate the concept of context-dependent efficacy, M_2 receptor signaling induced by dualsteric compounds was analyzed in recombinant and native M_2 receptor expression systems, i.e. CHO-hM_2 and human lung fibroblasts (MRC-5), respectively. Taken together, detailed molecular pharmacology and physiology studies with dualsteric ligands pinpoint a novel approach for pharmacological selectivity, i.e. engineered context-sensitive signaling of G protein-coupled receptors (GPCRs).

MATERIALS AND METHODS

Test compounds

Oxotremorine M iodide (OxoM), pilocarpine hydrochloride (Pilo), atropine sulphate, *N*-methylscopolamine bromide, isoprenaline hydrochloride (ISO), metoprolol tartrate, forskolin (FSK), isobutylmethylxanthine (IBMX) and hemicholinium were obtained from Sigma-Aldrich Chemie (Steinheim, Germany). [^{3}H]N-methylscopolamine bromide ([^{3}H]NMS) and [^{3}H]choline were purchased from PerkinElmer Life and Analytical Sciences (Homburg, Germany).

The dualsteric agonists were kindly provided from Prof. DeAmici and Prof. Holzgrabe. Synthesis of the dualsteric agonists iper-6-phth (I-6-p; (Antony et al., 2009)) and iper-8-phth (I-8-p; (Bock et al., 2012)) is described elsewhere.

Cell culture

We used Flp-In^{TM}-Chinese Hamster Ovary cells (R75807, Invitrogen) stably expressing the human M_2 receptor (CHO-hM_2) and the human lung fibroblast cell line MRC-5 (CCL-171, ATCC). Cell lines were used in experiments until reaching passage 50 and 10 for CHO-hM_2 and MRC-5, respectively. MRC-5 and CHO cells were negatively tested for mycoplasma contamination. Both cell lines were cultured as described previously (Schrage et al., 2013).

Animals

Wild-type mice (C57BL/6 and CD1 strain) of both sexes were used in the described experiments. Mice (Charles River; Sulzfeld, Germany) were housed in isolated ventilated cages at 24°C with a 12:12-h light-dark cycle. Animals taken for organ and embryo isolation were killed by cervical dislocation. Animal experiments were approved by the responsible federal state authority (Landesamt fuer Natur-, Umwelt- und Verbraucherschutz Nordrhein-Westfalen).

JPET Fast Forward. Published on November 15, 2016 as DOI: 10.1124/jpet.116.237149
This article has not been copyedited and formatted. The final version may differ from this version.

[^{35}S]GTPγS accumulation

Preparation of membrane homogenates (CHO-hM_2) and [^{35}S]GTPγS binding experiments were conducted as described previously (Schrage et al., 2013). In short, homogenates of membranes from CHO-hM_2 wild-type cells (40 µg/ml) were incubated with 0.07 nM [^{35}S]GTPγS and agonist-induced [^{35}S]GTPγS incorporation was measured after 1 h. Experiments were performed in quadruplicate. A sample size of $n \geq 3$ was elected on grounds of earlier publications (Antony et al., 2009; Schröder et al., 2010; Schrage et al., 2013).

Inhibition of acetylcholine release

Superfusion studies on hippocampal brain slices of female eight-week old CD1 mice were performed as described earlier (Schulte et al., 2012). Briefly, slices (0.3 mm thick, diameter 2 mm) were preincubated with [^{3}H]choline (0.1 µM) for 30 min. Tissues were superfused at 37°C for 110 min with oxygenated physiological salt solution containing 3.25 mM calcium and 10 µM hemicholinium to block high-affinity choline uptake. Agonist was added from 60 min of superfusion onwards. Two periods of electrical field stimulation for 2 min (3 Hz, 200 mA, 2 ms) were applied after 40 min (S_1) and 90 min (S_2) of superfusion. Fractional rates of tritium overflow without (S_1) and with agonist (S_2) were calculated and agonist-induced inhibition of transmitter release finally expressed as S_2/S_1 ratio. OxoM and I-6-p were tested on brain slices obtained from three and seven independent isolations, respectively. Pilo was tested in a supramaximal concentration of 1 mM on two brain slices obtained from the same isolation.

Beating frequency of cardiomyocytes

JPET Fast Forward. Published on November 15, 2016 as DOI: 10.1124/jpet.116.237149
This article has not been copyedited and formatted. The final version may differ from this version.

Atrial cardiomyocytes were enzymatically isolated by collagenase treatment according to Fleischmann et al. (Fleischmann et al., 2004) from murine embryonic mid-stage hearts (mouse strain CD1; sex of the used embryo "unknown"). After isolation on day 13.5-16.5 from female pregnant mice, cells were plated on sterile gelatine-coated glass coverslips and kept in the incubator (37 °C, 5% CO_2) for 48 h. On the day of experiment, coverslips were transferred into a temperature-controlled recording device (37 °C) and superfused with increasing agonist-containing buffer solution (140 mM NaCl, 5.4 mM KCl, 1 mM $MgCl_2$, 1.8 mM $CaCl_2$, 10 mM HEPES and 10 mM glucose; pH 7.4 with NaOH). As cellular read-out, the negative chronotropic effect in spontaneously beating cardiomyocytes was measured by videomicroscopy as described previously (Dobrowolski et al., 2008). Movies of beating cardiomyocytes were recorded with a Sony XCD-X710 camera at 30 frames/s, and beating areas were analyzed off-line with a custom-written software (Labview 7.1 and IMAQ, National Instruments, Austin, TX, USA). Test compound effect was determined as the average frequency over the last 30 s in steady-state and was normalized to baseline frequency. Each agonist was tested at least in three independent experiments.

Cardiomyocyte sarcomere shortening

Ventricular cardiomyocytes were prepared from male adult mouse hearts (mouse strain C57BL/6, age: 20-25 weeks) as described previously (Tiemann et al., 2003) and kept in oxygenated Tyrode's solution (135 mM NaCl, 4 mM KCl, 1 mM $MgCl_2$, 1.8 mM $CaCl_2$, 2 mM HEPES; 9 mM glucose, BSA 1 mg/ml and trypsin inhibitor 0.017 mg/ml; pH 7.4 with NaOH) at room temperature until use. Cells were allowed to attach to laminin-coated microscope slides and stimulated externally with 40 V for 0.4 ms. Sarcomere shortening was measured under a pacing frequency of 2 Hz at 36 °C in absence and presence of 1 µM ISO. Subsequently, isolated cardiomyocytes were superfused with ISO-containing muscarinic

JPET Fast Forward. Published on November 15, 2016 as DOI: 10.1124/jpet.116.237149
This article has not been copyedited and formatted. The final version may differ from this version.

agonist solutions. Agonists were tested in a concentration of 10 µM and shortening recordings evaluated by calculating the mean of five shortenings in the steady state. Sarcomere shortening was recorded using a video imaging system and SarcLen software (IonOptix; Milton, MA, USA). The effect of the tested agonists was normalized to the effect of ISO and plotted in a bar diagram. OxoM and I-6-p were tested in cardiomyocytes of at least four different isolations.

Left ventricular catheter measurements (LVCM)

Measurements were performed as described previously (Wenzel et al., 2012). Briefly, female mice (age: 8-12 weeks) of the CD1 strain were anesthetized by inhalation of 1% isoflurane and 0.6 l/min O_2. The right carotid artery was exposed and a small catheter (1F, Millar) was inserted through an incision and placed into the left ventricle. OxoM, I-6-p (0.4 µmol/kg each) or metoprolol (3 mg/kg) were injected into the left jugular vein. Left ventricular pressure was recorded continuously via the Millar Aria 1 system connected to a PowerLab A/D converter (AD Instruments, Spechbach, Germany). For analysis maximal systolic pressures and the heart rate before and 2 min after injection were compared. Based on earlier publications (Barocelli et al., 2001; El Beheiry et al., 2011), a sample size of $n \geq 5$ was elected. Experiments were performed without randomization; no blinding was performed.

Dynamic Mass Redistribution (DMR)

To detect GPCR signaling on whole-cell level in CHO-hM_2 and MRC-5, we used label-free biosensor technology based on dynamic mass redistribution (DMR) (Schröder et al., 2010). The principle of DMR was described elsewhere in detail for CHO (Schröder et al., 2011) and MRC-5 cells (Lamyel et al., 2011). Experiments were conducted in Hank's balanced Salt Solution (HBSS; 14025, Invitrogen) buffer supplemented with 20 mM HEPES (pH 7.0) at 28 °C. DMR responses of CHO-hM_2 and MRC-5 were quantified using the agonist-induced

JPET Fast Forward. Published on November 15, 2016 as DOI: 10.1124/jpet.116.237149
This article has not been copyedited and formatted. The final version may differ from this version.

maximal response between 0 and 1800 seconds.In CHO-hM_2, agonists were additionally tested in presence of 10 µM FSK. Independent experiments were performed in triplicate. As reported previously for CHO cells (Schröder et al., 2011), concentration-effect curves of MRC-5 were almost independent from the time point of DMR reading (supplementary Fig. S5). Independent experiments were conducted at least three times in triplicate or quadruplicate according to earlier publications (Schröder et al., 2010; Bock et al., 2012; Schrage et al., 2013).

Radioligand binding assays

[^{3}H]NMS dissociation assay: Two-point [^{3}H]NMS dissociation experiments with membrane homogenates expressing muscarinic receptors were conducted in 5 mM $NaKP_i$ buffer (4 mM Na_2HPO_4, 1 mM KH_2PO_4, pH 7.4) at 23 °C as described previously (Huang et al., 2005). Preparation of membrane homogenates (CHO and MRC-5) and cardiac tissue homogenates (murine ventricular tissue from adult C57BL/6 mice; age and sex "unknown") was conducted according to Schrage et al. (Schrage et al., 2013) and Keller et al. (Keller et al., 2015), respectively.

[^{3}H]NMS] competition assay: Whole cells experiments using CHO-hM_2 and MRC-5 cells were conducted in Hank's balanced Salt Solution (HBSS; 14025, Invitrogen) buffer supplemented with 20 mM HEPES (pH 7.0) at 28 °C as described previously for MRC-5 (Schrage et al., 2013).

Radioligand binding experiments were conducted at least three times in duplicate; sample size was elected on grounds of earlier publications (Bock et al., 2012; Schrage et al., 2013).

cAMP determination

Intracellular cAMP of CHO-hM_2 and MRC-5 cells was determined using the HTRF®-cAMP dynamic kit (Cisbio, Bagnols-sur-Cèze Cedex, France) following the manufacturer's

JPET Fast Forward. Published on November 15, 2016 as DOI: 10.1124/jpet.116.237149
This article has not been copyedited and formatted. The final version may differ from this version.

instructions with the following modification: Experiments were performed in absence of IBMX to avoid interference with basal cAMP. Experiments were conducted in Hank's balanced Salt Solution (HBSS; 14025, Invitrogen) buffer supplemented with 20 mM HEPES (pH 7.0), as the DMR experiments. Fluorescence was quantified on a Mithras LB 940 reader (Berthold Technologies, Bad Wildbad, Germany). A cAMP standard curve with the final concentrations of 0, 0.17, 0.69, 2.78, 11.1, 44.5, 178 and 712 nM cAMP was tested to define the measurement window of the assay (supplementary Fig. S3A). Then, cellular cAMP was related to the protein content of the cells determined according to Lowry using human serum albumin as a standard (Lowry et al., 1951). Experiments were performed in triplicate using cells in suspension.

Statistics and data analysis

Data are shown as mean values ± standard error of the mean (SEM) for n independent observations. F-tests were performed to check the variance between statistically tested groups; no difference was detected. Based on the assumption of normal data distribution, comparison of means was performed using Student's two-side *t*-tests (paired and unpaired) or one-way analysis of variance (ANOVA). ANOVA was followed by Dunnett's or Tukey's post-test, as appropriate, with $p < 0.05$ taken as significant.

All data were analyzed using Prism 6.0 (GraphPad Software, San Diego, CA, USA). Functional and binding data were analyzed using a four-parameter logistic function yielding the inflection point (IC_{50}), the upper and lower plateau, and the slope factor of the curves. In case of functional experiments, the inflection point represents the potency (EC_{50}) and the upper plateau describes the maximal inducible effect (E_{max}). If the observed slope factors did not differ significantly from unity (F-test, $p > 0.05$), the slope factor was constrained to 1.

JPET Fast Forward. Published on November 15, 2016 as DOI: 10.1124/jpet.116.237149
This article has not been copyedited and formatted. The final version may differ from this version.

In case of [^{3}H]NMS competition binding experiments, IC_{50} values were converted to apparent binding constants (K_A) using the Cheng-Prusoff correction (Cheng and Prusoff, 1973). Receptor density (B_{max}) was calculated from IC_{50} values according to DeBlasi et al. (DeBlasi et al., 1989).

Additionally, mean values from DMR experiments with CHO-hM_2 and MRC-5 cells were analyzed by the operational model of agonism (Black and Leff, 1983) to estimate the coupling efficiency as described earlier (Rajagopal et al., 2011; Schrage et al., 2013) with K_A fixed to the agonist's dissociation binding constant estimated from whole cell radioligand binding experiments (supplementary Tab. S2):

$$E = \frac{E_{max} \times \tau \times [A]}{\tau \times [A] + ([A] + K_A)} \qquad (1)$$

In this equation, E is the response, E_{max} is the maximal response of the system (determined by the full agonist OxoM), τ is the coupling efficacy between the agonist/receptor complex and its downstream signaling partners, K_A is the agonist's dissociation binding constant, and [A] is the concentration of agonist.

The maximum effect of an agonist predicted from the coupling efficiency was calculated according to equation 2 (Black et al., 2010) and plotted as a theoretical curve in Fig. 5 (lower panel) with E_{max} of the system fixed to 1.

$$\underset{A \to \infty}{E} = \frac{E_{max} \times \tau}{\tau + 1} \qquad (2)$$

JPET Fast Forward. Published on November 15, 2016 as DOI: 10.1124/jpet.116.237149
This article has not been copyedited and formatted. The final version may differ from this version.

RESULTS

The cellular context determines the intensity of muscarinic M_2 receptor signaling

Ligands are traditionally subdivided in full agonists, partial agonists or antagonists depending on their ability to elicit a receptor-mediated physiological or pharmacological response (Stephenson, 1956). It is important to note that the amount of detectable receptor activation is system- and assay dependent (Langmead and Christopoulos, 2013). In systems with high receptor density and/or assays with significant signal amplification, full and partial agonists can induce the same maximum effect (Rajagopal et al., 2011; Schrage et al., 2015). Therefore, we determined the intrinsic efficacy of muscarinic agonists first in an assay with low signal amplification using receptor homogenates of CHO-hM_2 cells. [^{35}S]GTPγS-accumulation is a functional readout to detect inhibitory G protein activation that is close to the receptor and directly linked to the agonist-induced receptor activation (Fig. 1A) (Milligan, 2003). The orthosteric activator OxoM is known to be as effective as acetylcholine and represents a full agonist (Schrage et al., 2013). Pilo is known to induce less G protein activation via the M_2 receptor than OxoM (VanGelderen et al., 1996) and was employed as a "partial agonist". In contrast to OxoM, which elicited maximal G protein activation, Pilo and the prototypal dualsteric agonist I-6-p induced only effects of 60 ± 3% and 75 ± 3%, respectively (Fig. 1B). The potency for receptor mediated [^{35}S]GTPγS incorporation was similar for OxoM and I-6-p, whereas Pilo was found to be less effective (Fig. 1B pEC_{50}: 8.07 ± 0.19 for OxoM, 7.49 ± 0.26 for I-6-p and 5.80 ± 0.12 for Pilo). However, the quantification of agonist-induced G protein activation in a particular cellular system (in this case CHO-hM_2) does not allow for deriving pharmacological parameters of agonist behavior in a different cellular context.

To analyze the effect of muscarinic agonists in native cellular systems with dominant M_2 receptor expression, we used murine hippocampal brain slices and murine embryonic cardiomyocytes (eCM) to determine inhibitory muscarinic autoreceptor function and the muscarinic-mediated negative chronotropic effect, respectively. In the central nervous system

JPET Fast Forward. Published on November 15, 2016 as DOI: 10.1124/jpet.116.237149
This article has not been copyedited and formatted. The final version may differ from this version.

(CNS), autoinhibition of acetylcholine release is primarily mediated via activation of presynaptic $G_{i/o}$-coupled muscarinic acetylcholine receptors which inhibit voltage-sensitive calcium channels that are involved in the regulation of neutrotransmitter release (Fig. 1C) (Caulfield, 1993; Shapiro et al., 1999). The M_2 receptor subtype is known to be the dominant muscarinic autoreceptor in the hippocampus (Zhang et al., 2002). As expected, all agonists failed to fully inhibit acetylcholine release in the hippocampal brain slices (Fig. 1D); even iperoxo, an agonist with supraphysiological efficacy (Schrage et al., 2013), did not fully inhibit acetylcholine release (Etscheid et al., 2014). Therefore, the effect of OxoM was considered as the maximum inducible effect in this system. Compared to OxoM, the dualsteric ligand I-6-p was clearly less effective and behaved as a weak partial agonist (Fig. 1D). Due to the already low effect of I-6-p, Pilo was only tested in the concentration of 1 mM and was as effective as I-6-p. In comparison to [^{35}S]GTPγS-accumulation experiments, potencies were shifted to higher concentrations but were again in the same range for OxoM and I-6-p (pEC_{50}: 6.58 ± 0.27 and 4.79 ± 0.80 for OxoM and I-6-p, respectively). Because muscarinic acetylcholine receptor activation is also known to mediate dangerous slowing of the heart rate (Fig. 1E), we next investigated the effect in cardiomyocytes. For this, we measured the agonist-induced negative chronotropic effect on spontaneous beating eCM by videomicroscopy. This assay is an indirect detection method for M_2 receptor activation (Fleischmann et al., 2004). Therefore, eCM were superfused with increasing concentrations of test compound. Cumulative administration of either the orthosteric activator OxoM, the partial agonist Pilo or the dualsteric agonist I-6-p caused concentration-dependent lowering of spontaneous beating rates (Fig. 1F). OxoM and I-6-p possessed similar potencies (pEC_{50}: 6.88 ± 0.10 and 6.62 ± 0.10 for OxoM and I-6-p, respectively) and showed full intrinsic efficacy. Even the less potent agonist Pilo (pEC_{50}: 5.21 ± 0.12) caused a complete arrest of spontaneous beating. Upon wash-out with agonist-free solution, all tested cells resumed spontaneous beating (OxoM: 94 ± 3 % (n=33), I-6-p: 80 ± 3% (n=34), Pilo: 64 ± 4% (n=36)).

JPET Fast Forward. Published on November 15, 2016 as DOI: 10.1124/jpet.116.237149
This article has not been copyedited and formatted. The final version may differ from this version.

In sum, the distinct efficacy profiles of the full agonist OxoM, the partial agonist Pilo and the dualsteric agonist I-6-p in three different expression systems (i.e. (i) membrane homogenates of CHO-hM_2 cells, (ii) hippocampal brain slices, and (iii) embryonic cardiomyocytes) nicely demonstrate the critical role of the cellular context with respect to full and partial agonism of ligands.

Dualsteric muscarinic agonist action is sensitive to intracellular cAMP in cardiomyocytes

In cardiomyocytes, activation of M_2 receptors leads to inhibition of the adenylyl cyclase via activation of $G_{i/o}$ proteins and hence inhibits formation of the second messenger cAMP (Brodde and Michel, 1999). Therefore, it is imaginable that the intensity of cellular read-out depends on the basal intracellular cAMP level. To check whether dualsteric agonist action is reduced in case of increased intracellular cAMP in eCM, I-6-p-induced decrease of eCM beating was tested under basal conditions and under sympathetic stimulation (Fig. 2). Real-time recordings are shown in the upper panels (Fig. 2A and 2B), whereas single data points are plotted in the lower panels (Fig. 2C and 2D). To mimic sympathetic stimulation, eCM were pretreated with the β-adrenergic agonist isoprenaline (ISO) in combination with the phosphodiesterase inhibitor isobutylmethylxanthine (IBMX). The combination of ISO (100 nM) and IBMX (100 µM) provides maximal stimulation of the system (Ji et al., 1999; Malan et al., 2004). Cardiomyocytes responded with an increase of spontaneous beating rate by at least 15% (15 out of 20 cells; responding cells were plotted in Fig. 2D and their individual response visualized via a connecting line). In comparison to baseline frequency, ISO induced a significant increase in beating frequency (basal: 139 ± 7 bpm vs. ISO/IBMX: 197 ± 11 bpm; mean values ± SEM, $p < 0.0001$, paired *t*-test). In the presence of ISO and IBMX, I-6-p failed to achieve full intrinsic efficacy even at concentrations of 10 µM (Fig. 2D). In contrast,

JPET Fast Forward. Published on November 15, 2016 as DOI: 10.1124/jpet.116.237149
This article has not been copyedited and formatted. The final version may differ from this version.

OxoM 10 µM could still completely suppress spontaneous beating. We checked our findings of dualsteric agonist action also in adult ventricular cardiomyocytes by measuring sarcomere shortening as an inotropic response. In the presence of ISO, I-6-p induced significantly less negative inotropy in these cells than the orthosteric agonist OxoM (supplementary Fig. S2). Taken together, these findings are in line with the hypothesis that a given adrenergic tone provides better protection against negative chronotropy and inotropy induced by the dualsteric muscarinic agonist I-6-p compared to the purely orthosteric agonist OxoM.

The dualsteric muscarinic agonist I-6-p engenders superior cardiovascular tolerability in vivo

Systemic administration of muscarinic agonists in mammals is known to cause a pronounced reduction of heart rate and mean arterial pressure (Barocelli et al., 2001; Takakura et al., 2003; Fisher et al., 2004). To check the cardiodepressive action of the orthosteric agonist OxoM and the dualsteric agonist I-6-p in vivo, left ventricular catheter measurements were carried out in anesthetized mice. Because of their permanent charge both compounds are unlikely to pass the blood-brain-barrier, which rules out central cardiodepressive effects. Both agonists were administered intravenously by bolus injection into the left jugular vein. OxoM was administered at a dose of 100 µg/kg to induce a maximal effect (Barocelli et al., 2001). Based on the mean body weight and blood volume of mice (i.e. 30 g and 4 ml, respectively), this will result in an initial blood concentration of 3 µM. The dualsteric agonist I-6-p was applied at the same concentration as OxoM as both compounds were equipotent in eCM (Fig. 1F).

Real-time recordings of left ventricular systolic pressure (LVSP, Fig. 3A and 3C) and heart rate (HR, Fig. 3B and 3D) revealed a pronounced suppression of cardiovascular function in the case of OxoM, whereas I-6-p was well tolerated. In particular, OxoM was lethal in 60% of the animals, whereas all mice of the I-6-p-group survived. Statistical analysis of cardiac

JPET Fast Forward. Published on November 15, 2016 as DOI: 10.1124/jpet.116.237149
This article has not been copyedited and formatted. The final version may differ from this version.

function showed that, starting from similar baseline levels of LVSP and HR, OxoM induced a significantly stronger cardiovascular depression in mice compared to the dualsteric agonist I-6-p (Fig. 3E vs. 3F; LVSP: reduction to 54 ± 6% (OxoM) vs. 90 ± 3% (I-6-p), $p < 0.001$; HR: reduction to 40 ± 5% (OxoM) vs. 86 ± 2% (I-6-p), $p < 0.001$). Due to the small effect of I-6-p, a second dose was administered 10 minutes after the first one. The second application induced no further effect, thus indicating that the applied concentration of I-6-p was maximally active (LVSP: reduction by 10 ± 3% (1st application) vs. reduction by 1 ± 2% (2nd application), HR: reduction by 14 ± 2% (1st application) vs. reduction by 2 ± 1% (2nd application)).

To check the basal β-adrenergic tone of anesthetized mice in our experiments, we applied the β-adrenoceptor blocker metoprolol by i.v.-injection (3 mg/kg according to El Beheiry et al. (El Beheiry et al., 2011)). Relative to baseline, treatment with metoprolol resulted in a LVSP of 90 ± 4% ($p > 0.05$, paired *t*-test) and a HR of 81 ± 2% ($p < 0.01$, paired *t*-test) (Fig. 3E and 3F), indicating a significant endogenous sympathetic tone in our experimental conditions. Therefore, we hypothesized that I-6-p showed better in vivo cardiovascular tolerability in mice because of a higher sensitivity to the endogenous β-sympathetic tone.

Intracellular cAMP mediates loss of sensitivity to dualsteric muscarinic agonists

Experiments on isolated cardiomyocytes and in anesthetized mice suggested that interventions to increase intracellular cAMP weaken cholinergic $G_{i/o}$-signaling in the case of the dualsteric ligand I-6-p. For the analysis and quantification of signaling efficiency, we took advantage of CHO cells as recombinant host to recapitulate this signaling paradigm by recombinant expression of the human muscarinic M_2 receptor subtype (CHO-hM_2, i.e. hM_2 "overexpression" system). Cells were studied in the absence and presence of forskolin (FSK), a direct activator of adenylyl cyclases (Seamon et al., 1981) that increased intracellular cAMP in a concentration-dependent manner (supplementary Fig. S3B) (supplementary Fig. S3C). After FSK-pretreatment (10 µM), that increased intracellular cAMP to the level in human

JPET Fast Forward. Published on November 15, 2016 as DOI: 10.1124/jpet.116.237149
This article has not been copyedited and formatted. The final version may differ from this version.

lung fibroblasts (MRC-5) (supplementary Fig. S3C and supplementary Tab. S1), we checked for potential effects of high intracellular cAMP levels on compound efficacy. MRC-5 were additionally applied which express the M_2 subtype endogenously (Matthiesen et al., 2006; Schrage et al., 2013). This was additionally verified by orthosteric [^{3}H]N-methylscopolamine ([^{3}H]NMS) dissociation experiments employing the allosteric inhibitor action of W84 (supplementary Fig. S4).

To quantify muscarinic agonist action on whole cell level in all three different cellular systems (i.e. CHO-hM_2, CHO-hM_2 + FSK, and MRC-5), we used the label-free optical biosensor Epic® and measured agonist-induced dynamic mass redistribution (DMR) in living cells (Schröder et al., 2010; Schröder et al., 2011); this is outlined in Fig. 4. To gain deeper insight into how the cellular context influences agonist efficiency, we included the middle-chain-elongated derivative iper-8-phth (I-8-p). I-8-p is characterized by an increased coupling efficiency at the expense of less signaling pathway-selectivity compared with I-6-p (Bock et al., 2012).

In CHO-hM_2 cells, muscarinic agonists induced positive DMR signals with a characteristic peak (real-time recordings, Fig. 4A) representing M_2 receptor activation (Bock et al., 2012). All tested ligands behaved as full agonists under basal conditions, as none of the compounds had a lower maximum effect than the full agonist OxoM (Fig. 4B). As reported previously, OxoM is as efficacious as the endogenous agonist acetylcholine (Schrage et al., 2013). In the presence of FSK, the absolute level of OxoM-induced DMR nearly doubled relative to control conditions. Additionally, DMR-signals fanned out and partial agonism emerged for I-6-p and Pilo (Fig. 4D), whereas efficacy of the middle chain-elongated dualsteric ligand I-8-p did not differ from the efficacy of OxoM (Fig. 4E).

In MRC-5 cells, test compounds revealed a similar pattern of full/partial-DMR-agonism as found with FSK-pretreated CHO-hM_2 cells (Fig. 4G and 4H). However, a switch from full to partial agonism was observed for I-8-p (Fig. 4H). Regarding the relative potency of each

JPET Fast Forward. Published on November 15, 2016 as DOI: 10.1124/jpet.116.237149
This article has not been copyedited and formatted. The final version may differ from this version.

agonist, inflection points (EC_{50}) were shifted to higher concentrations in the following order: CHO-hM_2 < CHO-hM_2 + FSK < MRC-5 (compare Fig. 4C, 4F, 4G and supplementary Tab. S2). A decrease of potency typically occurs when an agonist switches from full to partial agonism, because a rightward shift of the inflection point indicates a decline of spare receptors in the corresponding systems (Kenakin, 2007; Rajagopal et al., 2011).

Agonist-encoded coupling efficiency dictates context-sensitivity of action

Experimental findings suggested that the level of intracellular cAMP is critical for dualsteric ligand-induced M_2 receptor activation. Coupling efficiency (τ) determines whether and to which extent a ligand transforms from a full to a partial agonist upon a change of cellular context. Coupling efficiency is a measure that includes the efficacy of an agonist and the sensitivity of the system to agonism (Kenakin, 2007). To quantify coupling efficiency of the ligands applied in this study, data from DMR experiments (see above) were analyzed according to the operational model of agonism (Black and Leff, 1983) as described before (Rajagopal et al., 2011; Schrage et al., 2013). In Fig. 5, agonist coupling efficiency (as log τ) is plotted against the cellular context (upper panel) and the maximal response (E_{max}) of the agonists in the tested system (lower panel). The intracellular cAMP content and the receptor densities differ among the tested cellular systems (supplementary Tab. S1): CHO-hM_2 - low cAMP and high receptor density, CHO-hM_2 + FSK - high cAMP and high receptor density, MRC-5 - high cAMP and low receptor density. Ranking of the applied test compounds according to their coupling efficiencies (Fig. 5, upper panel) yielded a rather stable pattern irrespective of the cellular system: OxoM > I-8-p > I-6-p ~ Pilo. Under FSK-pretreatment and even more so in the MRC-5 context, coupling efficiency was reduced in case of each agonist compared to CHO-hM_2 control conditions (upper panel; represented by the vertical dashed lines). Most importantly, the maximum effect (Fig. 5, lower panel) was differently affected

depending on the individual starting level of coupling efficiency. In particular, E_{max} was hardly changed in case of OxoM, diminished with I-8-p only in the MRC-5 context, and profoundly reduced with Pilo and I-6-p, both in the CHO-hM_2 + FSK and the MRC-5 context. Taken together, the dualsteric building-block design opens an avenue for graded context-sensitive GPCR activation.

Data availability

All relevant data are available from the authors.

DISCUSSION

Muscarinic acetylcholine receptors (mAChRs) regulate the activity of numerous fundamental central and peripheral functions. Therefore, muscarinic agonists and antagonists possess several therapeutic indications and are currently approved for some clinical conditions (for reviews (Wess et al., 2007; Kruse et al., 2014)). However, the clinical usefulness of these agents is limited by side effects caused by the non-selective activation of all or multiple mAChRs. For example, therapeutic systemic administration of conventional muscarinic agonists is mainly hampered by central tremorgenic activity (Gomeza et al., 1999) and peripheral cardiac depression (Barocelli et al., 2001). It is well known that conventional full agonists evoke profound cardiovascular depression (Barocelli et al., 2001). It was therefore of particular interest that a novel type of GPCR-activator was recently introduced (Antony et al., 2009). Regarding the chemical design, this type of activator is a dualsteric compound consisting of an orthosteric and an allosteric building block, both linked via a hydrocarbon chain (chemical structure, supplementary Fig. S1).

Quantification of M_2 receptor-mediated signaling in three different cellular systems (i.e. (i) CHO-hM_2 cells, (ii) hippocampal brain slices, and (iii) embryonic cardiomyocytes) revealed that the intrinsic efficacy of I-6-p was highly system- and assay-dependent, whereas the efficacy of OxoM remained largely stable over all systems. In comparison to direct G protein activation quantified in [^{35}S]GTPγS binding experiments, the efficacy of I-6-p to inhibit neurotransmitter release from cholinergic nerve endings was relatively weak (cf Fig.1D), whereas spontaneous beating of eCM was completely suppressed (cf Fig.1F). This powerful effect in eCM might result from a high receptor reserve and/or a strong signal amplification in cardiomyocytes. The term receptor reserve (“spare receptors”) addresses the fraction of cellular receptors that is not needed for a maximum response of the system (Kenakin, 2013). Of note, we showed that the intrinsic efficacy of the dualsteric agonist I-6-p, in contrast to the

orthosteric agonist OxoM, is reduced under elevated intracellular cAMP in primary cardiomyocytes (Fig. 2 and supplementary Fig. S2).

Furthermore, I-6-p induced less cardiac depression in vivo compared to OxoM and did not induce cardiac arrest (Fig. 3). This good cardiac tolerability of I-6-p makes a clinical application of dualsteric muscarinic agonists more likely than initially expected. One potential indication for dualsteric ligands may be the treatment of pain disorders (Matera et al., 2014). Context-sensitive signaling offers a mechanistic explanation as to why the cardiovascular tolerability of I-6-p by far exceeded the tolerability of OxoM in anaesthetized mice. As described by various researchers before (Gehrmann et al., 2000; Rose et al., 2007; El Beheiry et al., 2011; Mabe and Hoover, 2011), application of the β-blocker metoprolol revealed a significant β-adrenergic tone acting on the mouse heart in our experiments. In consequence, β_1-adrenergic signaling stimulates basal formation of intracellular cAMP in cardiomyocytes. In contrast, muscarinic antagonists have no significant effect on basal HR in mice (Wickman et al., 1998; Mabe and Hoover, 2011).

Ranking of the applied test compounds according to their coupling efficiencies shows a stable pattern irrespective of the cellular system: OxoM > I-8-p > I-6-p ~ Pilo (Fig. 5 and supplementary Tab. S3). Agonists with weak coupling efficiency have to activate more receptors for a given response than efficient activators. Thus, the system has a lower receptor reserve for such agonists. In particular, dualsteric (orthosteric/allosteric) agonists lose their receptor reserve under conditions of high intracellular cAMP (compare Fig. 4, I-6-p in panel B with panel E). This is not due to a reduction in absolute receptor number but due to an increased number of receptors which have to be activated to induce the maximum response of the system. If the intracellular cAMP level is increased, a stronger M_2-signaling is needed to induce a similar effect than in systems with low cAMP levels. If high intracellular cAMP levels are combined with a low receptor density, as it is the case for MRC-5 cells, a switch

from full to partial agonism is also detectable for I-8-p (compare Fig. 4, I-8-p in panel E with panel H). If receptor reserve is exhausted, partial agonism emerges.

In case of CHO-hM_2, the sensitivity of the system to agonism was diminished by an increase of intracellular cAMP induced by FSK. As a consequence, compounds with lowest coupling efficiency in CHO-hM_2 were the first that switched from full to partial agonism after FSK-pretreatment (Fig. 5 lower panel: half-filled circles of Pilo (grey) and I-6-p (red)). In case of MRC-5, besides high intracellular cAMP, additionally receptor density was reduced (supplementary Tab. S1). As a consequence, not only Pilo and I-6-p, but additionally I-8-p became a partial agonist (Fig. 4 lower panel, open circles of Pilo (grey), I-6-p (red) and I-8-p (green)).

Taken together, we suggest the following mechanism of context-dependent coupling efficiency: Under conditions of low cAMP levels, a small fraction of activated M_2 receptors will suffice to counterbalance cAMP-mediated actions: high "M_2 receptor reserve" – even M_2 agonists with low signaling efficiency such as Pilo are able to generate a maximum muscarinic effect. With increasing cAMP levels to be counteracted, an increasing fraction of M_2 receptors needs to be activated: reduced sensitivity of the system to agonism or, in other words, less "receptor reserve". This mechanism can also be described as "functional antagonism", if cAMP is increased due to adrenergic counter-regulation (Pyne et al., 1992). A compound with less intrinsic efficacy for receptor activation, i.e. lower coupling efficiency, such as I-6-p and Pilo then fail to induce full agonism. Pilo behaved similar to I-6-p, but is able to pass the blood-brain-barrier and may exert central nervous side effects such as seizures (Bymaster et al., 2003).

Furthermore, the design of partial agonists in the past seemed to be fairly random. Now, the novel dualsteric concept allows the design of tailor-made agents for the exploitation of context-dependent signaling via linkage of orthosteric/allosteric building blocks and variation

of the length of the hydrocarbon middle chain (Antony et al., 2009; Bock et al., 2012; Bock et al., 2014).

Irrespective of specific therapeutic perspectives, our study shows that pharmacological modulators can be designed which are sensitive to the functional context of a target. Commonly, pharmacologically targeted receptors such as the muscarinic acetylcholine receptor species, are classified into subtypes depending on differences in structure (for reviews (Haga, 2013; Kruse et al., 2014)). Exploitation of context-dependent signaling expands the repertoire for selective pharmacological intervention in that one and the same receptor subtype may reveal different pharmacological phenotypes depending on the functional state of the cell population that harbors the receptor.

In conclusion, dualsteric (orthosteric/allosteric) targeting of muscarinic acetylcholine receptors generates new forms of pharmacological modulation and selectivity. Dualsteric agents were first characterized as signaling pathway-selective ("biased") activators of muscarinic receptors (Antony et al., 2009; Bock et al., 2012). Very recently, the dualsteric design concept was exploited to achieve the first designed dynamic partial agonists in the field of G protein-coupled receptors (Bock et al., 2014). Here we introduce context-sensitive signaling as an important mechanism of pharmacological selectivity for clinical application, and we show that capacity to monitor cell function in real time both *in vitro* and *in vivo* was key to discovery of this.

ACKNOWLEDGEMENT

We thank Corning Inc. for their support on the Epic® system.

Competing interests

The authors declare that they have no competing interests.

AUTHORSHIP CONTRIBUTIONS

Participated in research design: Seemann, Wenzel, Schrage, Sasse, Holzgrabe, Schlicker, Kostenis, Fleischmann, Mohr

Conducted experiments: Seemann, Wenzel, Etscheid, Bödefeld, Bartol

Contributed new agents and analytic tools: Warnken, Klöckner, Holzgrabe, DeAmici, Schlicker, Racké, Kostenis, Meyer, Fleischmann, Mohr

Performed data analysis: Seemann, Wenzel, Schrage, Mohr

Wrote or contributed to the writing of the manuscript: Seemann, Wenzel, Schrage, Etscheid, Warnken, Holzgrabe, DeAmici, Schlicker, Racké, Kostenis, Meyer, Fleischmann, Mohr

REFERENCES

Antony J, Kellershohn K, Mohr-Andrä M, Kebig A, Prilla S, Muth M, Heller E, Disingrini T, Dallanoce C, Bertoni S, Schrobang J, Tränkle C, Kostenis E, Christopoulos A, Höltje HD, Barocelli E, De Amici M, Holzgrabe U and Mohr K (2009) Dualsteric GPCR targeting: a novel route to binding and signaling pathway selectivity. *FASEB J* 23:442-450.

Barocelli E, Ballabeni V, Bertoni S, De Amici M and Impicciatore M (2001) Evidence for specific analgesic activity of a muscarinic agonist selected among a new series of acetylenic derivatives. *Life Sci* 68:1775-1785.

Black JW and Leff P (1983) Operational models of pharmacological agonism. *Proc R Soc Lond B Biol Sci* 220:141-162.

Black JW, Leff P, Shankley NP and Wood J (2010) An operational model of pharmacological agonism: the effect of E/[A] curve shape on agonist dissociation constant estimation. 1985. *Br J Pharmacol* 160 Suppl 1:S54-64.

Bock A, Chirinda B, Krebs F, Messerer R, Bätz J, Muth M, Dallanoce C, Klingenthal D, Tränkle C, Hoffmann C, De Amici M, Holzgrabe U, Kostenis E and Mohr K (2014) Dynamic ligand binding dictates partial agonism at a G protein-coupled receptor. *Nat Chem Biol* 10:18-20.

Bock A, Merten N, Schrage R, Dallanoce C, Bätz J, Klöckner J, Schmitz J, Matera C, Simon K, Kebig A, Peters L, Müller A, Schrobang-Ley J, Tränkle C, Hoffmann C, De Amici M, Holzgrabe U, Kostenis E and Mohr K (2012) The allosteric vestibule of a seven transmembrane helical receptor controls G-protein coupling. *Nat Commun* 3:1044.

Brodde OE and Michel MC (1999) Adrenergic and muscarinic receptors in the human heart. *Pharmacol Rev* 51:651-690.

Bymaster FP, Carter PA, Yamada M, Gomeza J, Wess J, Hamilton SE, Nathanson NM, McKinzie DL and Felder CC (2003) Role of specific muscarinic receptor subtypes in

cholinergic parasympathomimetic responses, in vivo phosphoinositide hydrolysis, and pilocarpine-induced seizure activity. *Eur J Neurosci* 17:1403-1410.

Caulfield MP (1993) Muscarinic receptors--characterization, coupling and function. *Pharmacol Ther* 58:319-379.

Cheng Y and Prusoff WH (1973) Relationship between the inhibition constant (K1) and the concentration of inhibitor which causes 50 per cent inhibition (I50) of an enzymatic reaction. *Biochem Pharmacol* 22:3099-3108.

DeBlasi A, O'Reilly K and Motulsky HJ (1989) Calculating receptor number from binding experiments using same compound as radioligand and competitor. *Trends Pharmacol Sci* 10:227-229.

Dobrowolski R, Sasse P, Schrickel JW, Watkins M, Kim JS, Rackauskas M, Troatz C, Ghanem A, Tiemann K, Degen J, Bukauskas FF, Civitelli R, Lewalter T, Fleischmann BK and Willecke K (2008) The conditional connexin43G138R mouse mutant represents a new model of hereditary oculodentodigital dysplasia in humans. *Hum Mol Genet* 17:539-554.

El Beheiry MH, Heximer SP, Voigtlaender-Bolz J, Mazer CD, Connelly KA, Wilson DF, Beattie WS, Tsui AK, Zhang H, Golam K, Hu T, Liu E, Lidington D, Bolz SS and Hare GM (2011) Metoprolol impairs resistance artery function in mice. *J Appl Physiol (1985)* 111:1125-1133.

Etscheid J, Mohr K and Schlicker E (2014) Iperoxo is a superpotent agonist at native presynaptic muscarinic M2 and M4 receptors in the mouse hippocampus and striatum. *Naunyn Schmiedebergs Arch Pharmacol* 387.

Fisher JT, Vincent SG, Gomeza J, Yamada M and Wess J (2004) Loss of vagally mediated bradycardia and bronchoconstriction in mice lacking M2 or M3 muscarinic acetylcholine receptors. *FASEB J* 18:711-713.

Fleischmann BK, Duan Y, Fan Y, Schoneberg T, Ehlich A, Lenka N, Viatchenko-Karpinski S, Pott L, Hescheler J and Fakler B (2004) Differential subunit composition of the G protein-activated inward-rectifier potassium channel during cardiac development. *J Clin Invest* 114:994-1001.

Gehrmann J, Hammer PE, Maguire CT, Wakimoto H, Triedman JK and Berul CI (2000) Phenotypic screening for heart rate variability in the mouse. *Am J Physiol Heart Circ Physiol* 279:H733-740.

Gomeza J, Shannon H, Kostenis E, Felder C, Zhang L, Brodkin J, Grinberg A, Sheng H and Wess J (1999) Pronounced pharmacologic deficits in M2 muscarinic acetylcholine receptor knockout mice. *Proc Natl Acad Sci U S A* 96:1692-1697.

Haga T (2013) Molecular properties of muscarinic acetylcholine receptors. *Proc Jpn Acad Ser B Phys Biol Sci* 89:226-256.

Harvey RD and Belevych AE (2003) Muscarinic regulation of cardiac ion channels. *Br J Pharmacol* 139:1074-1084.

Huang XP, Prilla S, Mohr K and Ellis J (2005) Critical amino acid residues of the common allosteric site on the M2 muscarinic acetylcholine receptor: more similarities than differences between the structurally divergent agents gallamine and bis(ammonio)alkane-type hexamethylene-bis-[dimethyl-(3-phthalimidopropyl)ammonium]dibromide. *Mol Pharmacol* 68:769-778.

Ji GJ, Fleischmann BK, Bloch W, Feelisch M, Andressen C, Addicks K and Hescheler J (1999) Regulation of the L-type Ca2+ channel during cardiomyogenesis: switch from NO to adenylyl cyclase-mediated inhibition. *FASEB J* 13:313-324.

Keller K, Maass M, Dizayee S, Leiss V, Annala S, Koth J, Seemann WK, Muller-Ehmsen J, Mohr K, Nurnberg B, Engelhardt S, Herzig S, Birnbaumer L and Matthes J (2015) Lack of Galphai2 leads to dilative cardiomyopathy and increased mortality in beta1-adrenoceptor overexpressing mice. *Cardiovasc Res* 108:348-356.

Kenakin T (2007) Functional selectivity through protean and biased agonism: who steers the ship? *Mol Pharmacol* 72:1393-1401.

Kenakin T (2013) New concepts in pharmacological efficacy at 7TM receptors: IUPHAR review 2. *Br J Pharmacol* 168:554-575.

Kruse AC, Kobilka BK, Gautam D, Sexton PM, Christopoulos A and Wess J (2014) Muscarinic acetylcholine receptors: novel opportunities for drug development. *Nat Rev Drug Discov* 13:549-560.

Kruse AC, Ring AM, Manglik A, Hu J, Hu K, Eitel K, Hübner H, Pardon E, Valant C, Sexton PM, Christopoulos A, Felder CC, Gmeiner P, Steyaert J, Weis WI, Garcia KC, Wess J and Kobilka BK (2013) Activation and allosteric modulation of a muscarinic acetylcholine receptor. *Nature* 504:101-106.

Lamyel F, Warnken-Uhlich M, Seemann WK, Mohr K, Kostenis E, Ahmedat AS, Smit M, Gosens R, Meurs H, Miller-Larsson A and Racké K (2011) The beta2-subtype of adrenoceptors mediates inhibition of pro-fibrotic events in human lung fibroblasts. *Naunyn Schmiedebergs Arch Pharmacol* 384:133-145.

Langmead CJ and Christopoulos A (2013) Supra-physiological efficacy at GPCRs: superstition or super agonists? *Br J Pharmacol* 169:353-356.

Lowry OH, Rosebrough NJ, Farr AL and Randall RJ (1951) Protein measurement with the Folin phenol reagent. *J Biol Chem* 193:265-275.

Mabe AM and Hoover DB (2011) Remodeling of cardiac cholinergic innervation and control of heart rate in mice with streptozotocin-induced diabetes. *Auton Neurosci* 162:24-31.

Malan D, Ji GJ, Schmidt A, Addicks K, Hescheler J, Levi RC, Bloch W and Fleischmann BK (2004) Nitric oxide, a key signaling molecule in the murine early embryonic heart. *FASEB J* 18:1108-1110.

Matera C, Flammini L, Quadri M, Vivo V, Ballabeni V, Holzgrabe U, Mohr K, De Amici M, Barocelli E, Bertoni S and Dallanoce C (2014) Bis(ammonio)alkane-type agonists of

muscarinic acetylcholine receptors: synthesis, in vitro functional characterization, and in vivo evaluation of their analgesic activity. *Eur J Med Chem* 75:222-232.

Matthiesen S, Bahulayan A, Kempkens S, Haag S, Fuhrmann M, Stichnote C, Juergens UR and Racké K (2006) Muscarinic receptors mediate stimulation of human lung fibroblast proliferation. *Am J Respir Cell Mol Biol* 35:621-627.

Milligan G (2003) Principles: extending the utility of [35S]GTP gamma S binding assays. *Trends Pharmacol Sci* 24:87-90.

Mohr K, Schmitz J, Schrage R, Tränkle C and Holzgrabe U (2013) Molecular alliance-from orthosteric and allosteric ligands to dualsteric/bitopic agonists at G protein coupled receptors. *Angew Chem Int Ed Engl* 52:508-516.

Nelson CP and Challiss RA (2007) "Phenotypic" pharmacology: the influence of cellular environment on G protein-coupled receptor antagonist and inverse agonist pharmacology. *Biochem Pharmacol* 73:737-751.

Pyne NJ, Grady MW, Shehnaz D, Stevens PA, Pyne S and Rodger IW (1992) Muscarinic blockade of beta-adrenoceptor-stimulated adenylyl cyclase: the role of stimulatory and inhibitory guanine-nucleotide binding regulatory proteins (Gs and Gi). *Br J Pharmacol* 107:881-887.

Rajagopal S, Ahn S, Rominger DH, Gowen-MacDonald W, Lam CM, Dewire SM, Violin JD and Lefkowitz RJ (2011) Quantifying ligand bias at seven-transmembrane receptors. *Mol Pharmacol* 80:367-377.

Rose RA, Kabir MG and Backx PH (2007) Altered heart rate and sinoatrial node function in mice lacking the cAMP regulator phosphoinositide 3-kinase-gamma. *Circ Res* 101:1274-1282.

Schrage R, De Min A, Hochheiser K, Kostenis E and Mohr K (2015) Superagonism at G protein-coupled receptors and beyond. *Br J Pharmacol*.

Schrage R, Seemann WK, Klöckner J, Dallanoce C, Racké K, Kostenis E, De Amici M, Holzgrabe U and Mohr K (2013) Agonists with supraphysiological efficacy at the muscarinic M2 ACh receptor. *Br J Pharmacol* 169:357-370.

Schröder R, Janssen N, Schmidt J, Kebig A, Merten N, Hennen S, Müller A, Blättermann S, Mohr-Andra M, Zahn S, Wenzel J, Smith NJ, Gomeza J, Drewke C, Milligan G, Mohr K and Kostenis E (2010) Deconvolution of complex G protein-coupled receptor signaling in live cells using dynamic mass redistribution measurements. *Nat Biotechnol* 28:943-949.

Schröder R, Schmidt J, Blättermann S, Peters L, Janssen N, Grundmann M, Seemann W, Kaufel D, Merten N, Drewke C, Gomeza J, Milligan G, Mohr K and Kostenis E (2011) Applying label-free dynamic mass redistribution technology to frame signaling of G protein-coupled receptors noninvasively in living cells. *Nat Protoc* 6:1748-1760.

Schulte K, Steingruber N, Jergas B, Redmer A, Kurz CM, Buchalla R, Lutz B, Zimmer A and Schlicker E (2012) Cannabinoid CB1 receptor activation, pharmacological blockade, or genetic ablation affects the function of the muscarinic auto- and heteroreceptor. *Naunyn Schmiedebergs Arch Pharmacol* 385:385-396.

Seamon KB, Padgett W and Daly JW (1981) Forskolin: unique diterpene activator of adenylate cyclase in membranes and in intact cells. *Proc Natl Acad Sci U S A* 78:3363-3367.

Shapiro MS, Loose MD, Hamilton SE, Nathanson NM, Gomeza J, Wess J and Hille B (1999) Assignment of muscarinic receptor subtypes mediating G-protein modulation of Ca(2+) channels by using knockout mice. *Proc Natl Acad Sci U S A* 96:10899-10904.

Stephenson RP (1956) A modification of receptor theory. *Br J Pharmacol Chemother* 11:379-393.

Takakura AC, Moreira TS, Laitano SC, De Luca Junior LA, Renzi A and Menani JV (2003) Central muscarinic receptors signal pilocarpine-induced salivation. *J Dent Res* 82:993-997.

Tiemann K, Weyer D, Djoufack PC, Ghanem A, Lewalter T, Dreiner U, Meyer R, Grohe C and Fink KB (2003) Increasing myocardial contraction and blood pressure in C57BL/6 mice during early postnatal development. *Am J Physiol Heart Circ Physiol* 284:H464-474.

VanGelderen JG, Daeffler L, Scherrer D, Mousli M, Landry Y and Gies JP (1996) M(2)-muscarinic receptors: How does ligand binding affinity relate to intrinsic activity? *Journal of Receptor and Signal Transduction Research* 16:135-148.

Wenzel D, Koch M, Matthey M, Heinemann JC and Fleischmann BK (2012) Identification of a novel vasoconstrictor peptide specific for the systemic circulation. *Hypertension* 59:1256-1262.

Wess J, Eglen RM and Gautam D (2007) Muscarinic acetylcholine receptors: mutant mice provide new insights for drug development. *Nat Rev Drug Discov* 6:721-733.

Wickman K, Nemec J, Gendler SJ and Clapham DE (1998) Abnormal heart rate regulation in GIRK4 knockout mice. *Neuron* 20:103-114.

Zhang W, Basile AS, Gomeza J, Volpicelli LA, Levey AI and Wess J (2002) Characterization of central inhibitory muscarinic autoreceptors by the use of muscarinic acetylcholine receptor knock-out mice. *J Neurosci* 22:1709-1717.

FOOTNOTES

a) [#]W.K.S. was supported by the North-Rhine Westphalia International Graduate Research School BIOTECH-PHARMA at the University of Bonn.

b) Part of this work was presented in an abstract form as follows: Seemann W, Wenzel D, Sasse P, Warnken M, Kostenis E, Racké K, Fleischmann B, Mohr K (2011) Dualsteric GPCR-targeting: Whole cell response to M2 receptor activation is cell type-dependent. *Naunyn-Schmiedebergs Arch Pharmacol* 381 (Suppl 1)

c) Wiebke Kirsten Seemann

Thieboldsgasse 3

50676 Cologne (Germany)

email:seemannwiebke@web.de

d) numbered footnotes: none

FIGURE LEGENDS

Figure 1: *System-dependence of agonist-induced M_2 receptor activation.* Shown are simplified illustrations of the tested systems (upper panels) and the corresponding concentration-effect curves of OxoM, Pilo and I-6-p (lower panels). The green triangles represent muscarinic agonists and the red-labeled terms the detected readouts of the corresponding assays. All data are means ± SEM of n independent experimental days. **(A, D):** G protein activation was quantified in [^{35}S]GTPγS binding experiments. **(B, E):** Inhibition of acetylcholine release was detected in adult murine hippocampal brain slices. Pilo (1 mM) was tested on two brain slices obtained from the same preparation (0.79, 0.81). Fig. 1C is modified from (Schulte et al., 2012). **(E, F):** Reduction of spontaneous beating was measured in isolated embryonic cardiomyocytes isolated from murine atria.

Figure 2: *Chronotropic response to muscarinic agonists in spontaneously beating murine embryonic atrial cardiomyocytes (eCM).* Increasing concentrations of the muscarinic agonists were applied cumulatively and normalized to baseline frequency. All experiments were performed on at least three independent days; a minimum of three data points was conducted per concentration. **(A, B):** Shown are representative real-time recordings of spontaneously beating cells and their response to I-6-p under basal conditions (A) and in presence of sympathetic stimulation (B). The dotted lines represent cardiac arrest, i.e. zero bpm. The "wash-out" period is marked with grey arrows. **(C, D):** Increasing concentrations of I-6-p were applied under basal conditions (C) and in presence of 100 nM ISO and 100 µM IBMX (D). The dotted lines represent the mean basal frequency, i.e. 140 ± 4 bpm (n=34) and 139 ± 7 bpm (n=15) in case of Fig. 2C and D, respectively. The "wash-out" effect of each tested cell is marked in grey. The response of each individual cell to ISO and IBMX is visualized by a connecting line in Fig. 2D.

JPET Fast Forward. Published on November 15, 2016 as DOI: 10.1124/jpet.116.237149
This article has not been copyedited and formatted. The final version may differ from this version.

Figure 3: *Effects of OxoM and I-6-p on blood pressure and heart rate in anesthetized mice.* **(A, B):** Original traces of left ventricular systolic blood pressure (LVSP) and heart rate (HR) recorded in response to OxoM (0.4 µmol/kg). **(C, D):** Original traces of LVSP and HR recorded in response to I-6-p (0.4 µmol/kg). **(E, F):** Statistical analysis of changes in LVSP and HR, respectively, in response to either metoprolol (3 mg/kg), OxoM, or I-6-p. *p* values < 0.05 considered statistically significant according to the Student's *t*-tests (*** $p < 0.001$). The paired *t*-test was used to check the effect of metoprolol and the unpaired *t*-test to compare the interindividual effects of both test compounds, i.e. OxoM vs. I-6-p. Indicated data are means ± SEM of n independent experiments.

Figure 4: *DMR response of CHO-hM$_2$, CHO-hM$_2$ after forskolin-pretreatment (+FSK), and MRC-5.* **(A, D, G)**: Indicated are representative real-time recordings of muscarinic agonist-induced DMR traces. The arrow marks the addition of the test compound after baseline read. **(B, E, H):** Bar graphs show mean maximal DMR responses of supramaximal agonist concentrations (OxoM: 100 µM, I-6-p: 100 µM, I-8-p: 10 µM, Pilo: 100 µM). Compared to OxoM, all ligands were tested for partial agonism; *p* values < 0.05 considered statistically significant according to one-way analysis of variance (ANOVA) with Dunnett's correction for comparison to OxoM (** $p < 0.01$). Indicated data are means ± SEM of at least n independent experiments. Experiments were performed in triplicate or quadruplicate. **(C, F, I)**: Concentration-effect curves of the tested ligands resulting from DMR assays. The dashed lines mark the inflection-points (pEC_{50}) of the tested ligands in case of CHO-hM$_2$. Indicated data are means ± SEM of at least three independent experiments. Experiments were performed in triplicate or quadruplicate. Potencies are listed in supplementary Tab. S2 for CHO-hM$_2$, CHO-hM$_2$ + FSK and MRC-5.

Figure 5: *Context-sensitive $G_{i/o}$-signaling of muscarinic M_2 receptor agonists.* **Upper panel:** Coupling efficiency of agonist-bound receptors to induce dynamic mass redistribution in

living cells is reflected by log τ-values for CHO-hM_2 cells under basal conditions, for CHO-hM_2 after FSK-pretreatment to elevate intracellular cAMP, and for MRC-5 fibroblasts with high endogenous cAMP and a minor receptor reserve. Test compounds are designated by the indicated colour code. Inclined stippled lines visualize context-dependent shifts of respective test compound coupling efficiency. Coupling efficiencies (log τ) were calculated according to equation 1 with K_A fixed to the agonist's dissociation binding constant (supplementary Tab. S3). **Lower panel:** Maximum effects (E_{max}) of the depicted agonists under the respective conditions (CHO-hM_2, CHO-hM_2 + FSK, MRC-5) expressed as a fraction of the respective system's maximum response set to E_{max} = 1. E_{max} values of the tested compounds were taken from DMR recordings (Fig. 4B: CHO-hM_2, 4E: CHO-hM_2 + FSK, 4H: MRC-5). Coupling efficiencies correspond to log τ-values shown in the upper panel. E_{max} and log τ-values are mean values ± SEM. The curve indicates the theoretical dependence of the maximum effect "E_{max}" from the coupling efficiency "log τ" calculated on the basis of equation 2. Of note, steepness and thus context-sensitivity of agonist action is highest at the inflection point of the E_{max}/log τ-relationship. Indicated are means ± SEM of at least three independent experimental days; further details are listed in supplemtary Tab. S3.

Figure 1

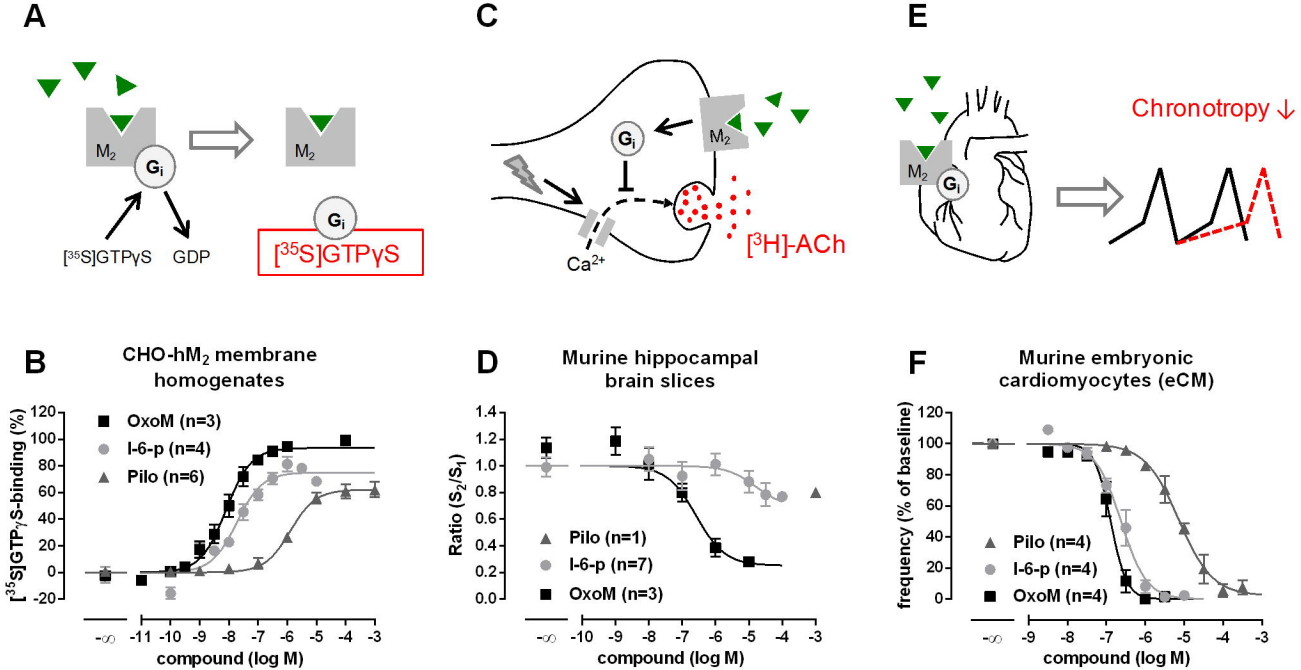
A
M2
Gi
[35S]GTPγS
GDP
M2
Gi
[35S]GTPγS
C
Gi
M2
Ca2+
[3H]-ACh
E
M2
Gi
Chronotropy ↓
B
CHO-hM2 membrane homogenates
[35S]GTPγS-binding (%)
OxoM (n=3)
I-6-p (n=4)
Pilo (n=6)
compound (log M)
D
Murine hippocampal brain slices
Ratio (S2/S1)
Pilo (n=1)
I-6-p (n=7)
OxoM (n=3)
compound (log M)
F
Murine embryonic cardiomyocytes (eCM)
frequency (% of baseline)
Pilo (n=4)
I-6-p (n=4)
OxoM (n=4)
compound (log M)

Figure 2

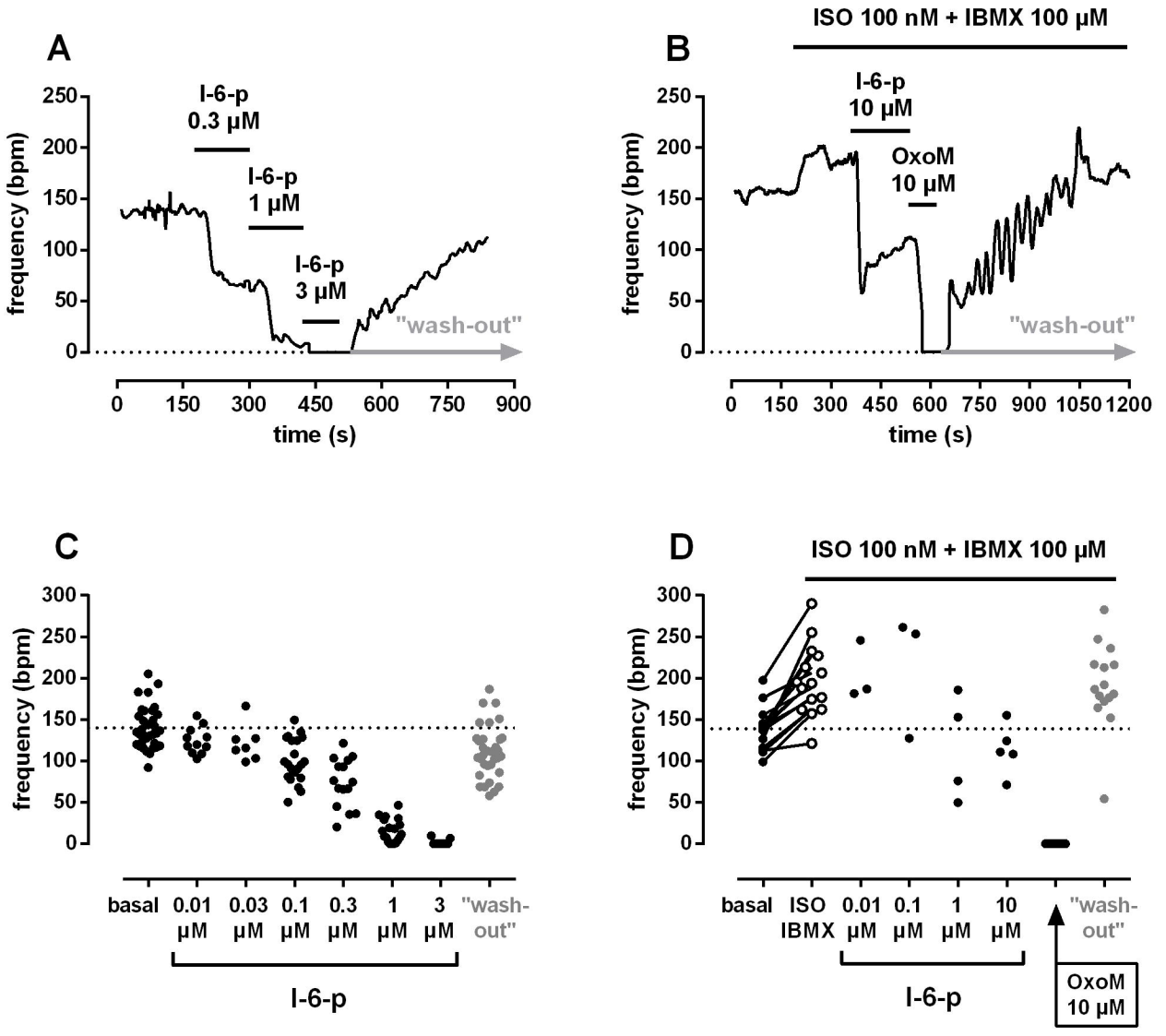
A
I-6-p
0.3 µM
I-6-p
1 µM
I-6-p
3 µM
"wash-out"
frequency (bpm)
time (s)
B
ISO 100 nM + IBMX 100 µM
I-6-p
10 µM
OxoM
10 µM
"wash-out"
frequency (bpm)
time (s)
C
frequency (bpm)
basal
0.01 µM
0.03 µM
0.1 µM
0.3 µM
1 µM
3 µM
"wash-out"
I-6-p
D
ISO 100 nM + IBMX 100 µM
frequency (bpm)
basal
ISO IBMX
0.01 µM
0.1 µM
1 µM
10 µM
"wash-out"
I-6-p
OxoM
10 µM

Figure 3

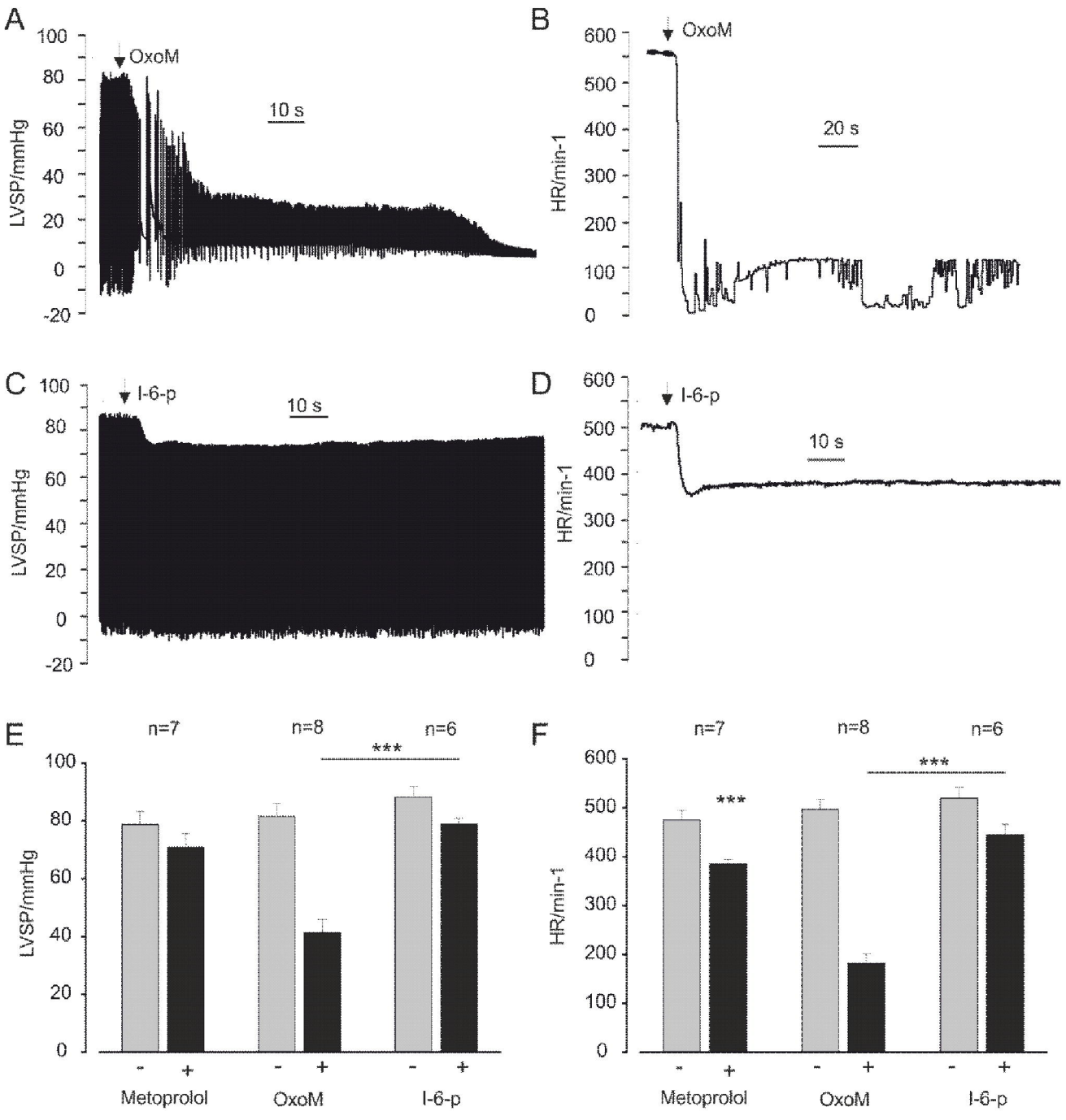
A
B
C
D
E
F
OxoM
I-6-p
10 s
20 s
LVSP/mmHg
HR/min-1
n=7
n=8
n=6
***
Metoprolol
OxoM
I-6-p
-
+

Figure 4

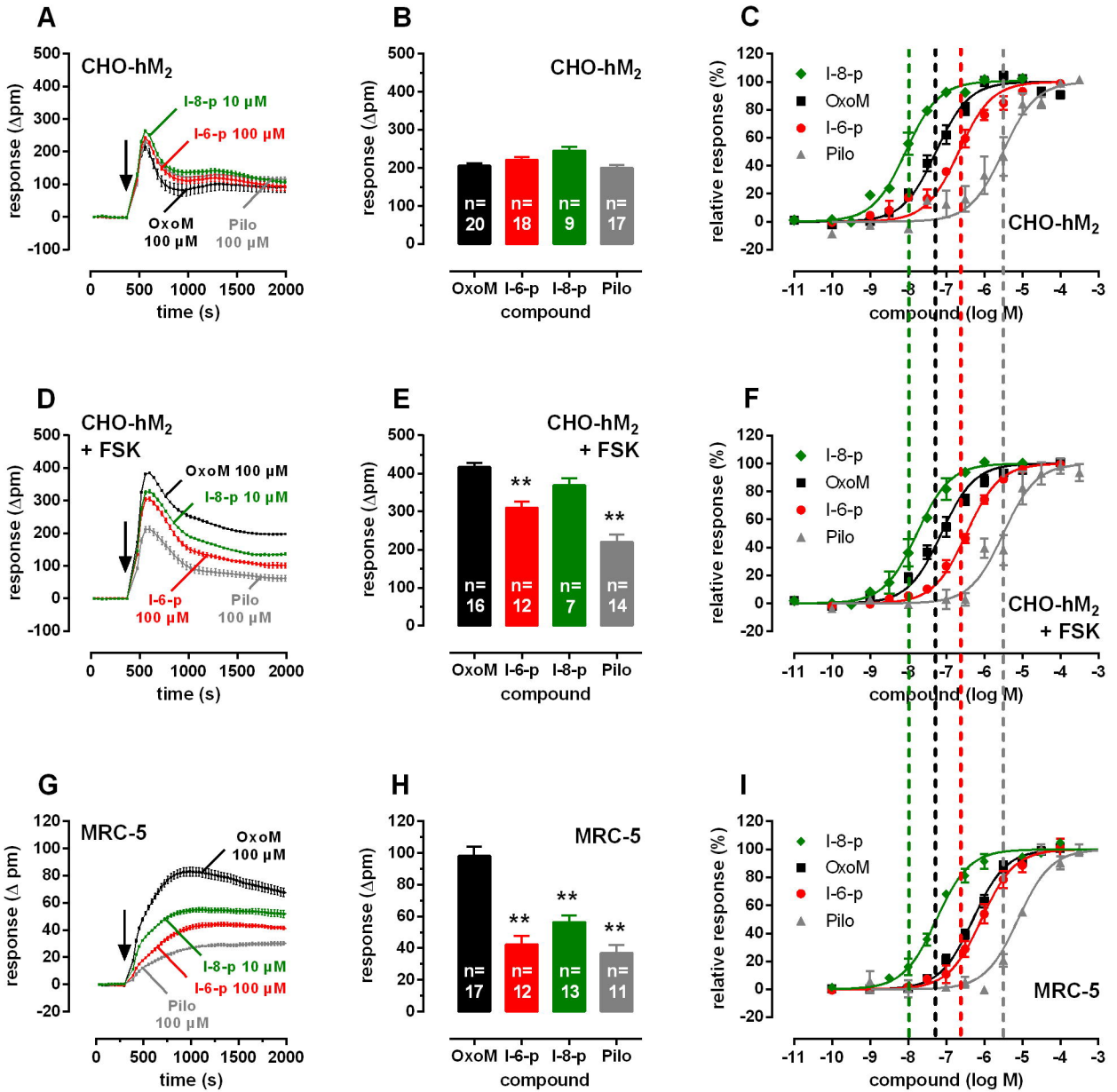
A
CHO-hM2
response (Δpm)
I-8-p 10 µM
I-6-p 100 µM
OxoM 100 µM
Pilo 100 µM
time (s)
B
CHO-hM2
response (Δpm)
n= 20
n= 18
n= 9
n= 17
OxoM I-6-p I-8-p Pilo
compound
C
relative response (%)
I-8-p
OxoM
I-6-p
Pilo
CHO-hM2
compound (log M)
D
CHO-hM2 + FSK
response (Δpm)
OxoM 100 µM
I-8-p 10 µM
I-6-p 100 µM
Pilo 100 µM
time (s)
E
CHO-hM2 + FSK
response (Δpm)
**
n= 16
n= 12
n= 7
n= 14
OxoM I-6-p I-8-p Pilo
compound
F
relative response (%)
I-8-p
OxoM
I-6-p
Pilo
CHO-hM2 + FSK
compound (log M)
G
MRC-5
response (Δ pm)
OxoM 100 µM
I-8-p 10 µM
I-6-p 100 µM
Pilo 100 µM
time (s)
H
MRC-5
response (Δpm)
**
n= 17
n= 12
n= 13
n= 11
OxoM I-6-p I-8-p Pilo
compound
I
relative response (%)
I-8-p
OxoM
I-6-p
Pilo
MRC-5
compound (log M)

Figure 5

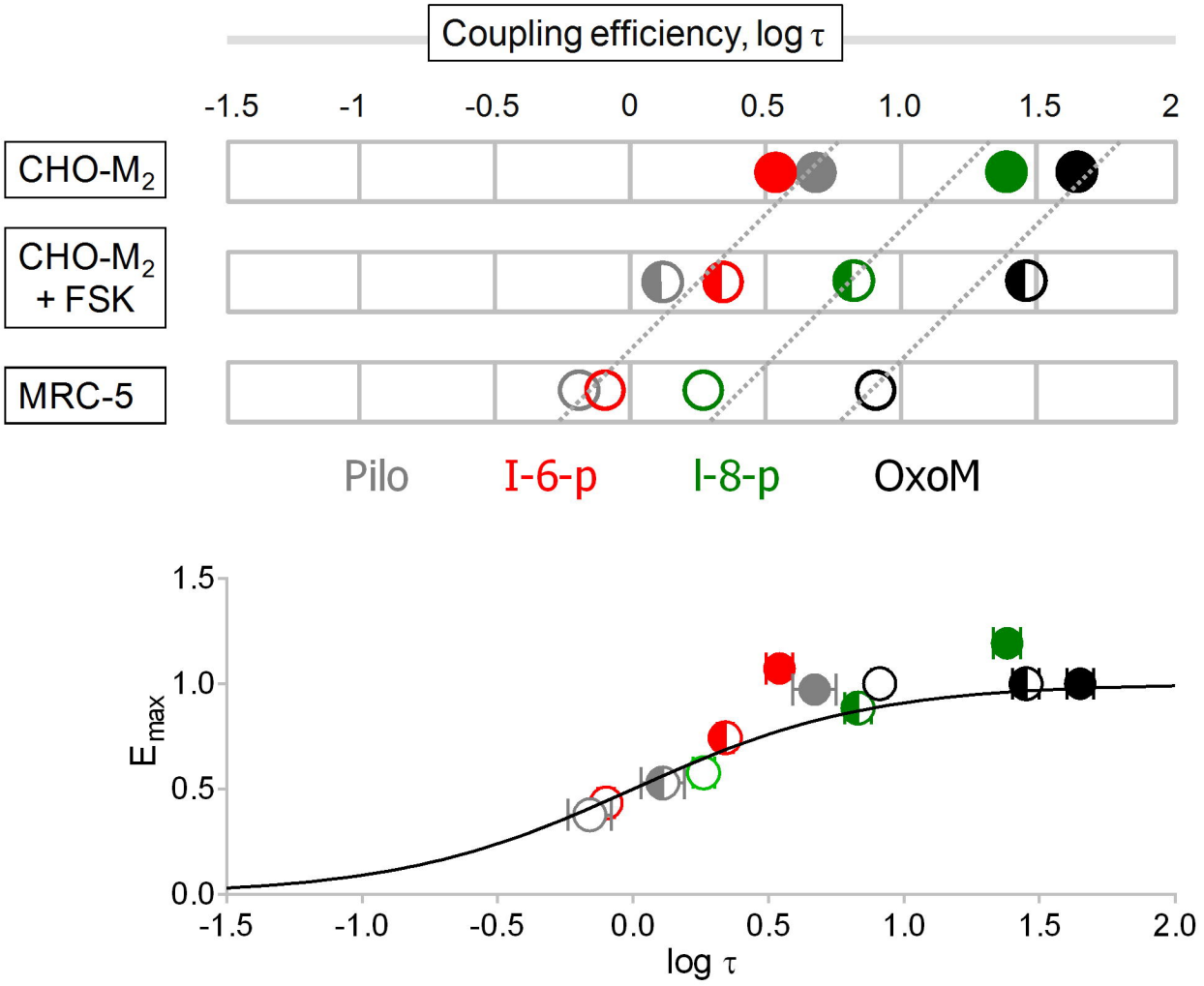
Coupling efficiency, log τ
-1.5
-1
-0.5
0
0.5
1.0
1.5
2
CHO-M2
CHO-M2 + FSK
MRC-5
Pilo
I-6-p
I-8-p
OxoM
Emax
1.5
1.0
0.5
0.0
-1.5
-1.0
-0.5
0.0
0.5
1.0
1.5
2.0
log τ

Supplementary Material

Engineered context-sensitive agonism – tissue-selective drug signaling through a G protein-coupled receptor

Wiebke K. Seemann, Daniela Wenzel, Ramona Schrage, Justine Etscheid, Theresa Bödefeld, Anna Bartol, Mareille Warnken, Philipp Sasse, Jessica Klöckner, Ulrike Holzgrabe, Marco DeAmici, Eberhard Schlicker, Kurt Racké, Evi Kostenis, Rainer Meyer, Bernd K. Fleischmann, and Klaus Mohr

Journal of Pharmacology and Experimental Therapeutics (JPET)

SUPPLEMENTARY FIGURES AND FIGURE LEGENDS

Supplementary figure S1:

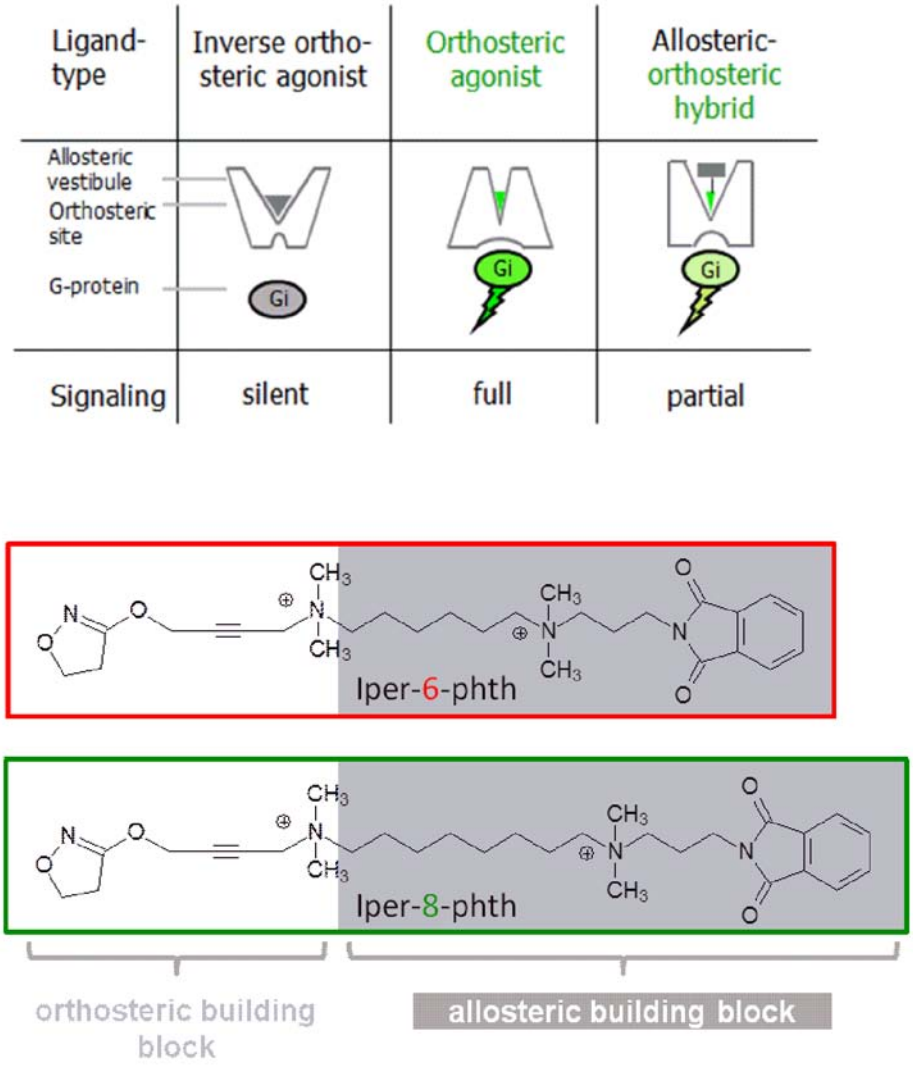

Supplementary figure S1: *Sketch of ligand structure-function-relationships in the muscarinic M_2 receptor.* **Upper panel:** According to crystal-structures (Kruse et al., 2013), the inactive-to-active-transition of the muscarinic M_2 receptor by acetylcholine-like agonists includes unfolding of the receptor's intracellular G_i protein binding site and corresponding narrowing of the extracellular entrance (vestibule) of the ligand binding pocket. Fusion of an

orthosteric agonist through a hydrocarbon linker chain with an appropriate inactive allosteric ligand (gray rectangle) yields a dualsteric (orthosteric/allosteric) hybrid with reduced signaling efficiency (Bock et al., 2012). **Lower panel (chemical structures):** The dualsteric agonists iper-6-phth (I-6-p; (Antony et al., 2009)) and iper-8-phth (I-8-p; (Bock et al., 2012)) consist of the orthosteric moiety iperoxo and a fragment of W84 as an allosteric building block linked via a hydrocarbon middle chain of either six or eight carbon atoms, respectively. With this hybrid design, only the dualsteric binding mode leads to receptor activation and downstream signaling.

Supplementary figure S2:

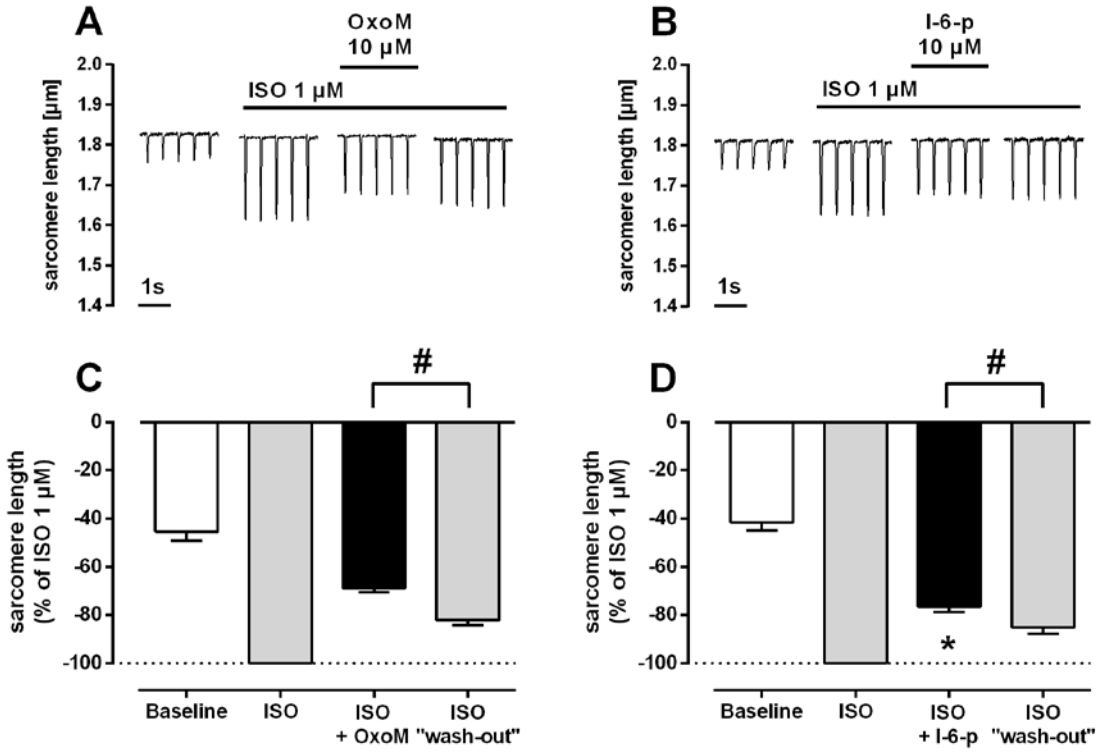

Supplementary figure S2*: Muscarinic agonist-induced cellular sarcomere shortening in mouse adult ventricular cardiomyocytes.* Sarcomere shortening was measured on individual, field-stimulated (2 Hz, 36 °C) cardiomyocytes under control conditions and in the presence of 1 µM ISO, because muscarinic agonists have little or no effect on ventricular function without adrenergic pre-stimulation (for reviews (Brodde and Michel, 1999; Harvey and Belevych, 2003)). Afterwards, the orthosteric agonist OxoM and the dualsteric agonist I-6-p were applied in a concentration of 10 µM in the continued presence of ISO. The applied agonist concentration of 10 µM provides maximum M_2 receptor activation in case of both, I-6-p and OxoM (Antony et al., 2009; Schrage et al., 2013). **(A, B):** Representative real-time recordings of sarcomere shortening in the steady-state for OxoM (A) and I-6-p (B). **(C, D):** Mean values of sarcomere shortening normalized to the shortening observed under ISO for OxoM (C) and I-6-p (D). In the presence of ISO, I-6-p induced significantly less negative inotropism than the

orthosteric agonist OxoM (Student's unpaired *t*-test, * $p < 0.05$). Upon "wash-out", sarcomere shortening did not completely recover from muscarinic agonist suppression. However, the effect was statistically significant (Student's paired *t*-test, # $p < 0.05$). Data are mean values ± SEM. The effect of OxoM was tested on 21 isolated cell obtained from 6 independent isolations. The effect of I-6-p was tested on 20 isolated cell obtained from 4 independent isolations.

Supplementary figure S3:

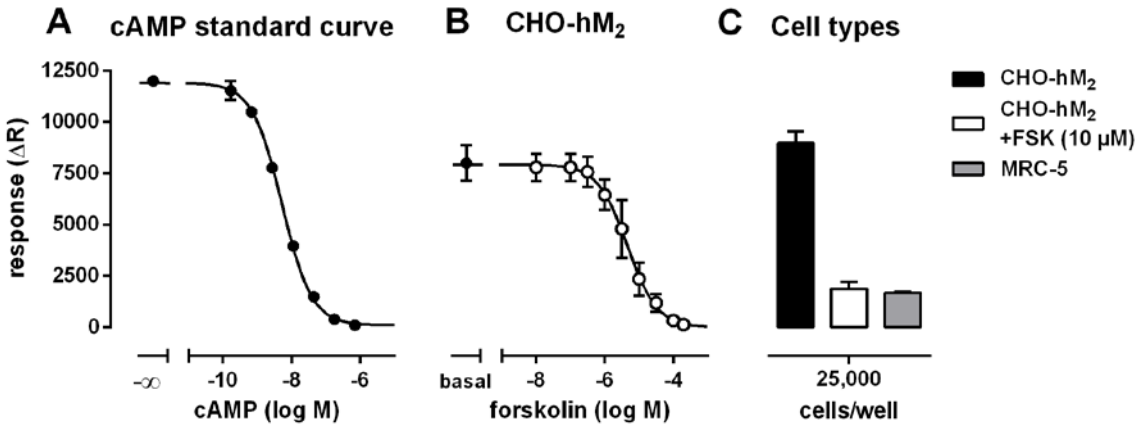

Supplementary figure S3: *FSK-induced increase of intracellular cAMP in CHO-hM$_2$.* Indicated are mean values ± SEM, n=2 (A), n=3 (B) and n=3-4 (C). Experiments were performed in triplicate. **(A):** The cAMP standard curve defines the measurement window of the cAMP assay. **(B):** The cell density of 50,000 cells/well was selected to check the effect of increasing concentrations of FSK. FSK increased the intracellular cAMP in a concentration-dependent manner and induced half maximal activation of the adenylyl cyclases at about 4 µM (pEC_{50}: -5.37 ± 0.18). **(C):** Comparison of different cell types was performed with 25,000 cells/well. Application of 10 µM FSK increased intracellular cAMP of CHO-hM$_2$ to the level detected in MRC-5.

Supplementary figure S4:

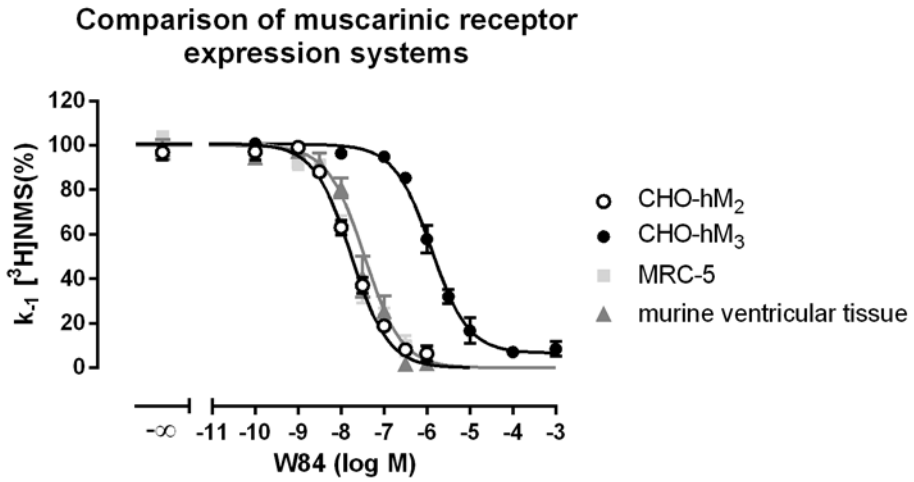

Supplementary figure S4: *Inhibition of [^{3}H]NMS dissociation by W84 at different cell- and tissue-based homogenates.* The allosteric modulator W84 had far higher affinity for [^{3}H]NMS-bound CHO-hM_2 (pEC_{50diss}: 7.76 ± 0.05, n=4) than CHO-hM_3 (pEC_{50diss}: 5.90 ± 0.06, n=4). As sensitivity for W84 of muscarinic receptors in MRC-5 cells (pEC_{50diss}: 7.77 ± 0.10, n=4) and murine ventricular tissue of C57BL/6 mice (pEC_{50diss}: 7.45 ± 0.11, n=5) matched sensitivity for CHO-hM_2, we conclude that the dominant receptor in the former is the M_2 subtype. Ordinate: Apparent rate constant (k_{-1}) of [^{3}H]NMS dissociation expressed as percentage of the control value in absence of W84. Abscissa: log concentration of W84. pEC_{50diss}: minus log concentration of W84 causing a half-maximal reduction of the rate constant of [^{3}H]NMS dissociation without allosteric compound. Indicated are mean values ± SEM; experiments were performed in duplicate on n independent experimental days.

Supplementary figure S5:

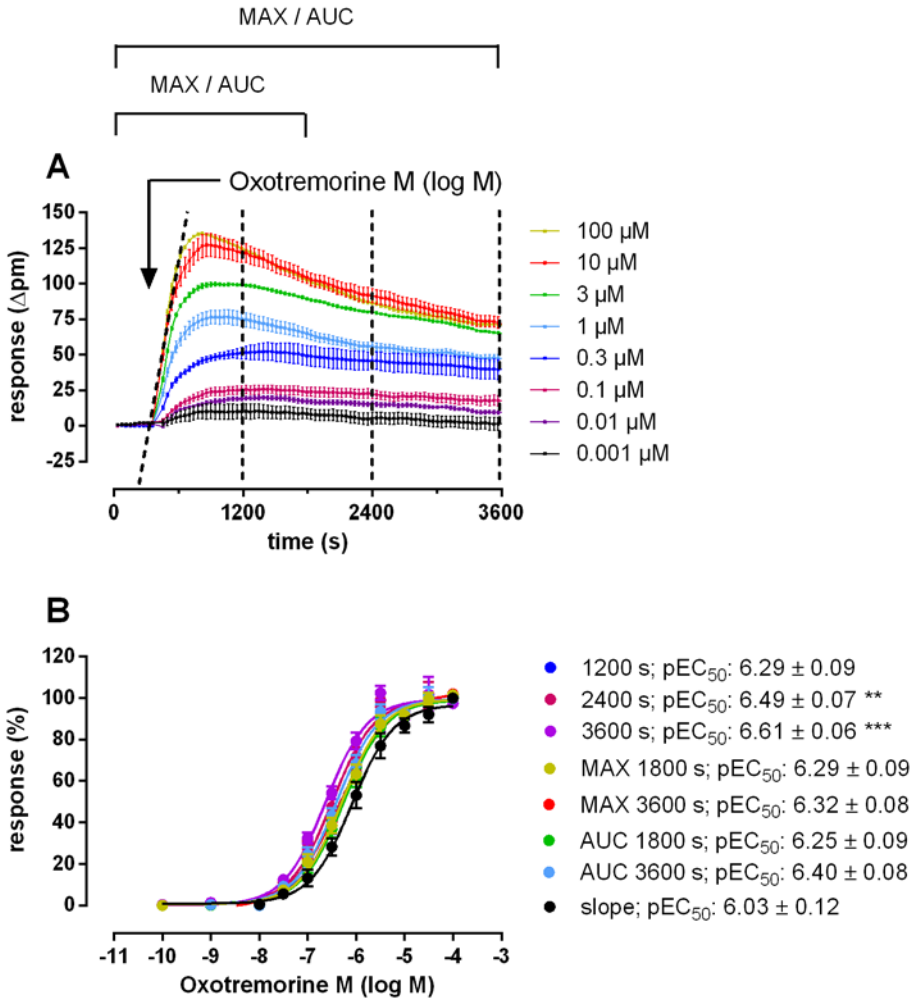

Supplementary figure S5: *Dynamic mass redistribution (DMR) analysis of MRC-5 cells and deduction of concentration-effect curves from DMR signals.* **(A):** Representative real-time recordings in MRC-5 (12,500 cells per well) stimulated with the indicated concentrations of the muscarinic agonist OxoM. **(B):** Concentration-effect curves resulting from different read-out parameters (*time of read-out*: "value 1200, 2400, 3600 s"; *maximum value within recording period* "MAX 1800, 3600 s"; *area under curve*, "AUC 1800, 3600 s"; *steepness of a tangent to the origin of the signal*, "slope") and the corresponding pEC_{50}-values (the –log concentrations at which agonists cause half-maximal responses). ** ($p < 0.01$), *** ($p < 0.001$) significantly different to the read-out "slope" according to One-way ANOVA with

Tukey's post test. Indicated are mean values ± SEM, n = 9. Experiments were performed in triplicate.

SUPPLEMENTARY TABLES

Supplementary table S1

Cell system	Surface receptors (fmol/mg protein)	Intracellular cAMP (pmol/mg protein)
CHO-hM_2	1071 ± 130 (n=11)	7 ± 1 (n=4)
CHO-hM_2 +FSK	892 ± 107 (n=11)	113 ± 40$^{\#\#}$ (n=3)
MRC-5	346 ± 59$^{***, ++}$ (n=8)	88 ± 3$^{\#}$ (n=4)

Supplementary table S1: *Cell surface receptors and intracellular cAMP content of CHO-hM_2, CHO-hM_2 +FSK and MRC-5.* Surface receptor numbers were significantly different between MRC-5 compared with both, CHO-hM_2 (*** $p < 0.001$) and CHO-hM_2 +FSK ($^{++}$ $p < 0.01$), but not between CHO-hM_2 and CHO-hM_2 + FSK. Intracellular cAMP levels were significantly different between MRC-5 and CHO-hM_2 ($^{\#}$ $p < 0.05$), as well as between CHO-hM_2 + FSK and CHO-hM_2 ($^{\#\#}$ $p < 0.01$), but not between MRC-5 and CHO-hM_2 + FSK. Data were tested according to one-way ANOVA and Tukey's multiple comparison test. Indicated data are means ± SEM of n independent experiments. Surface receptor determination and cAMP measurements were performed in duplicate and triplicate, respectively.

Supplementary table S2

Compound	Binding affinities (pK_A)			Potencies (pEC_{50})		
	CHO-hM_2	CHO-hM_2 (+FSK)	MRC-5	CHO-hM_2	CHO-hM_2 (+FSK)	MRC-5
OxoM	5.65 ± 0.03 (n=8)	5.71 ± 0.15 (n=4)	5.47 ± 0.09 (n=6)	7.27 ± 0.11 (n=8)	7.13 ± 0.11 (n=5)	6.29 ± 0.09 (n=9)
I-6-p	6.31 ± 0.06 (n=4)	6.39 ± 0.08 (n=4)	6.29 ± 0.05 (n=4)	6.67 ± 0.04 (n=3)	6.47 ± 0.07 (n=3)	6.15 ± 0.14 (n=4)
I-8-p	6.79 ± 0.21[a]	N.D.	N.D.	8.06 ± 0.07 (n=4)	7.77 ± 0.17 (n=3)	7.19 ± 0.11 (n=4)
Pilo	4.89 ± 0.11 (n=6)	4.77 ± 0.06 (n=4)	4.90 ± 0.07 (n=4)	5.51 ± 0.17 (n=4)	5.50 ± 0.22 (n=5)	5.10 ± 0.03 (n=3)

Supplementary table S2: *Binding affinities (pK_A* from whole cell binding experiments*)* and *potencies (pEC_{50}* from DMR experiments*) of the muscarinic agonists.* Data were obtained with CHO-hM_2 cells in absence and presence of forskolin (+FSK), and human lung fibroblasts (MRC-

5). Values represent the mean ± SEM of n independent experiments. Binding experiments were performed in duplicate and DMR experiments in triplicate or quadruplicate.

a value taken from Bock et al. (Bock et al., 2012). This value was also used to determine the coupling efficiency (τ) according to equation 1 for CHO-hM_2 + FSK and MRC-5, as binding affinities of OxoM, I-6-p and Pilo did not differ significantly in the different systems.

N.D. not determined

Supplementary table S3

log τ ($G_{i/o}$)	CHO-hM_2	CHO-hM_2 (+FSK)	MRC-5
OxoM	1.65 ±0.05 (n=5)	1.45 ±0.05 (n=5)	0.91 ±0.03 (n=9)
I-6-p	0.54 ± 0.05** (n=3)	0.34 ± 0.03** (n=3)	-0.10 ± 0.05** (n=4)
I-8-p	1.38 ± 0.05* (n=4)	0.83 ± 0.05** (n=3)	0.26 ± 0.04** (n=4)
Pilo	0.67 ± 0.08** (n=4)	0.11 ± 0.08** (n=5)	-0.16 ± 0.08** (n=3)

Supplementary table S3: *Coupling efficiencies (log tau; τ) of selected muscarinic agonists from DMR experiments.* Log τ-values were calculated for CHO-hM_2 cells under control conditions and after forskolin-pretreatment (+FSK) as well as for human lung fibroblasts (MRC-5) according to equation 1 with K_A fixed to the agonist's dissociation binding constant (supplementary Tab. S2). ** ($p < 0.01$), * ($p < 0.05$) significantly different to OxoM according to One-way ANOVA with Dunett's post test. Data are mean values ± SEM of n independent experiments.